INTERNATIONAL ATOMIC ENERGY AGENCY
UNITED NATIONS EDUCATIONAL, SCIENTIFIC AND CULTURAL ORGANIZATION
INTERNATIONAL CENTRE FOR THEORETICAL PHYSICS
I.C.T.P., P.O. BOX 586, 34100 TRIESTE, ITALY, CABLE: CENTRATOM TRIESTE

SMR.550 - 37

SPRING COLLEGE IN MATERIALS SCIENCE ON
"NUCLEATION, GROWTH AND SEGREGATION IN MATERIALS
SCIENCE AND ENGINEERING"
(6 May - 7 June 1991)

ORDERING OF VOIDS AND GAS BUBBLES IN RADIATION ENVIRONMENTS

K. KRISHAN
Materials Science Division
Department of Atomic Energy
Indira Gandhi Centre for Atomic Research
Tamilnadu
603102 Kalpakkam
India

Radiation Effects, 1982, Vol. 66, pp. 121–155
0033-7579/82/6604-0121$06.50

INVITED REVIEW ARTICLE

Ordering of Voids and Gas Bubbles in Radiation Environments

K. KRISHAN
Reactor Research Centre, Kalpakkam 603 102, Tamil Nadu, India

(Received May 17th, 1982)

SUMMARY

In this article the experimental and theoretical results on the formation of void and bubble lattices by irradiation are reviewed. The experimental observations are grouped into four categories: void lattices in metals formed by neutron and ion irradiation, void ordering by electron irradiation, bubble lattice formed by low energy light ion implantation, and void lattices in alkali earth fluorides. The article tries to develop a consistent physical picture for all these cases. The ordering is viewed mainly as a non-equilibrium phase transition and various mechanisms proposed for the instability are discussed and related to the observed kinetic conditions for ordering. The approach followed is consistent with other models based on crystal anisotropy and superlattice energy. The ordering therefore arises due to a combination of kinetic and energetic processes.

CONTENTS

1 ORDERED STRUCTURES IN SOLIDS

Symmetry manifests itself in a variety of ways when atoms combine to form solids. Atoms are known to arrange into periodic lattice structures and for near-equilibrium conditions give rise to beautiful shapes of crystals. In other cases, environment can influence the solidification process introducing non-equilibrium effects producing delightful shapes as in the case of snowflakes[1] or the dendritic tree-like patterns formed during solidification of alloys from their metals.[2] Symmetric arrangements involving atoms and defects can also form within the ordered host matrix of solids. These range from the faceted shapes of precipitates and voids due to crystallographic anisotropy to superlattice arrangement of defects. In the latter category are the well-known modulated structures[3] consisting of periodic arrangement of stacking faults, antiphase boundaries and shear planes in alloys and compounds like Cu_3Sn, Ni_3Mo, TiO_2 and ReO_3; superlattices consisting of vacancies and interstitials[4–6] in V_6N_5, $Ta_{64}C$, $V_{16}N$ and $Ta_{64}N$ respectively; periodic concentration fluctuations[7] due to electron irradiation in alloys like CuNi and irradiation induced superlattices of voids[8] and gas bubbles[9] in metals like Mo, Ni and compounds[10] like CaF_2. Environmental, equilibrium or non-equilibrium conditions play an important role in the emergence of these symmetric arrangements and the underlying mechanisms are varied and in some cases not well understood. This article deals mainly with ordering of voids and bubbles in radiation environments. However, there are parallels which can be drawn between radiation-induced ordering phenomena and ordering in other systems providing a useful contact with the different theoretical approaches. These general approaches are briefly discussed before dealing with specific questions regarding the formation of void and bubble lattices in radiation environments.

Most ordering phenomena can be traced to one or more of the following three mechanisms. (i) Near-equilibrium processes involving energy or entropy considerations, (ii) manifestation of crystallographic anisotropy effects, and (iii) non-equilibrium processes. The external shapes crystals acquire and the formation of modulated structures are near-equilibrium phenomena involving atomic and elastic interactions where crystallographic anisotropy plays an important role. Crystals form layer by layer through local atom additions, the external shapes corresponding to the slowest growing atomic planes.[11] In modulated structures like shear planes in TiO_2 (or ReO_3), electron microscopy reveals the early stages of the development and it is observed[12] that the shear planes form in pairs and develop by the co-operative rearrangement of atoms (cation interstitials in TiO_2 or ReO_3) on an active "hairpin" shaped front. The shear planes form with specific orientations like {132} or {121} in the host matrix, the latter being favoured for higher oxygen-deficient systems. The array develops by addition of shear planes in pairs until it extends throughout the crystal. Stoneham and Durham[13] have shown that the regular spacing between arrays is one where the long-range elastic strain and a small electrostatic interaction energy is a minimum. Similar elastic interaction has been proposed[14] for vacancy and interstitial lattices in Ta and V. Here it is impottant to observe that *local* atomic rearrangements determined by the crystal anisotropy interactions are involved in the formation of the ordered defect structure. On the other hand, we have the ordered patterns in snowflakes. These involve a *global* transformation where the entire symmetry pattern evolves spatially, simultaneously evolving through different stages.[2] There are no local or internal mechanisms which operate. The symmetric pattern arises when an instability develops due to the variation of some external parameter such as concentration or humidity. Such transformations involve non-equilibrium conditions and the instability arises due to the dynamic processes in the system while the specific symmetry which develops is influenced by the boundary conditions.

In many cases it is not possible on the basis of available experimental data to decide whether the ordered structure emerges purely by *local* energy considerations or involves *global* characteristics of non-equilibrium transitions. It is possible that the ordered structure which emerges may be influenced at different stages of its evolution by both these mechanisms. This perhaps may be the case with the ordering of voids and bubbles. It is for this reason that the theoretical models for void ordering have viewed the problem of void lattice formation from different points of view.† There are two striking features in the experimental observations regarding the ordering of voids and bubbles. Firstly, as a function of the radiation dose a random distribution of voids or bubbles is formed which only subsequently orders. Secondly, the ordered lattice is related or has the same symmetry and alignment as the host lattice. The first scenerio of a transformation from a disordered to an ordered lattice is very similar (at least superficially) to the self-organization process shown by several non-equilibrium dissipative systems.[16,17] Here the transition appears to have a global character with spatial alignments of voids appearing simultaneously at several places. These finally develop into a three-dimensional array as the system stabilizes after undergoing several instabilities as a function of some control parameter. However, in carrying this analogy further a basic difficulty appears in conceiving why the void or the bubble-lattice always emerges having the same symmetry as that of the host lattice. The rate equations used to model the evolution of the defect structure in radiation environments are homogeneous and hence spatially structureless. They contain no information about the crystal anisotropy and by themselves cannot provide any explanation about the void superlattice symmetry. At best, these equations can give information about the length scale for the spatial correlations based on the diffusion and the kinetic conditions for the onset of ordering but not the specific symmetry of the lattice. It is evident that this symmetry is not related to any external boundary conditions and therefore processes based on the crystallographic anisotropy must be important.

---

†An excellent discussion on the merits and demerits of these models is available in the reviews by A. M. Stoneham.[8,15]

At this stage it is instructive to look at the mechanisms involved in dendritic formations or snowflakes. In this case a characteristic length parameter is the ratio γ/L, where γ is the liquid–solid surface tension and L the latent heat per unit volume of the solid. The basic pattern emerges from the free-boundary conditions imposed on the solid–liquid interface which change with time as the interface progresses.[2] This gives the general features of the growth. However, the interesting aspect is that in this case also the crystalline anisotropy of the solid manifests itself in several ways; the orientation dependence of the surface tension γ, the anisotropy in the heat flow and the molecular attachment kinetics at the solid interface. The latter in the case of ice crystals restricts the growth to the basal plane giving snowflakes the flat feathering features.[2] We see, therefore, that in the process of ordering there is an intermingling of the basic kinetics involving a global non-equilibrium transition with local energy or anisotropy conditions.

From the above general introductory comments it is apparent that a complete understanding of all aspects of ordering of voids and bubbles is not yet available. However, different aspects like the kinetics of the transition, the emergence of the final structure, its stability and symmetry, can be viewed with the aid of different models with the hope that these can be integrated into a single mathematical structure. This is the approach which will be followed in this article. In Section 2 the basic phenomena and the available experimental results are reviewed. Section 3 deals with the kinetics of the transition viewed as a non-equilibrium dissipative system, while Section 4 sonsiders other models like those involving the interaction between voids and anisotropy effects. Finally, Section 5 concludes with a summary and comments about some of the outstanding problems.

2 THE PHENOMENA AND EXPERIMENTAL OBSERVATIONS

2.1 *The Phenomena*

The theory for the growth of voids in metals (random distribution) is now well established.[18–23] In its simplest form, in this theory, the radiation continuously produces vacancies and interstitials due to atomic displacements. These point defects subsequently undergo recombination (in pairs) or drift to sinks like dislocations, thereby maintaining a quasi-steady state concentration. The central concept is a *bias effect* whose origin can be traced to the difference in the strain fields associated with vacancies and interstitials which leads to a difference in their interaction with dislocations. This bias results in a slight preferential flow of interstitials to dislocations. As a consequence of this the vacancy concentration tends to increase since they are continuously produced together with the interstitials. However, the voids act as sinks for these vacancies and this explains why they grow in size as the irradiation continues. The two requirements of this theory are the existence of a biased interaction and the presence of a biased sink, namely dislocations. The model is schematically shown in Figure 1.

For practical application, the above model is an over-simplified one and other effects introduced by the radiation have to be taken into account.[20] The process of void formation in metals occurs at approximately $0.3T_m$, where T_m is the melting point of the metal. This is because the radiation-produced vacancies have to be mobile. Other defect structures can also develop as a result of the radiation. Two important ones are the interstitial dislocation loops and vacancy dislocation loops. The interstitial loops are formed as a result of clustering of interstitials (depending on temperature) and subsequently grow in the radiation environment. At high concentrations they can interact with each other, giving rise to a network dislocation structure. On the other hand, vacancy loops are formed due to an athermal collapse of the vacancy-rich core of cascades and later shrink by preferential interstitial absorption due to the bias. They therefore exist by a process of dynamic equilibrium being continuously produced athermally and subsequently shrinking in the environment of point defects. Vacancy loops are formed only by neutron and charged particle radiation and not by electron radiation, since in the latter case the atomic displacements result in Frenkel pairs and not in cascades.[20] There are also other effects which introduce additional complications in the detailed models. At high temperatures ($\gtrsim 0.3\,T_m$) thermal emission of vacancies is possible from the extended defects and in the case of vacancy loop contributes to a more rapid rate of shrinkage. Another variable involved is the concentration or number density of voids or interstitial loops. This generally increases with dose but tends to saturate at higher doses. These complex processes do not alter the basic mechanism of void evolution shown in Figure 1 but influence the rate of void growth at different temperatures. This is because the additional extended defects act as sinks and compete for the point defects.

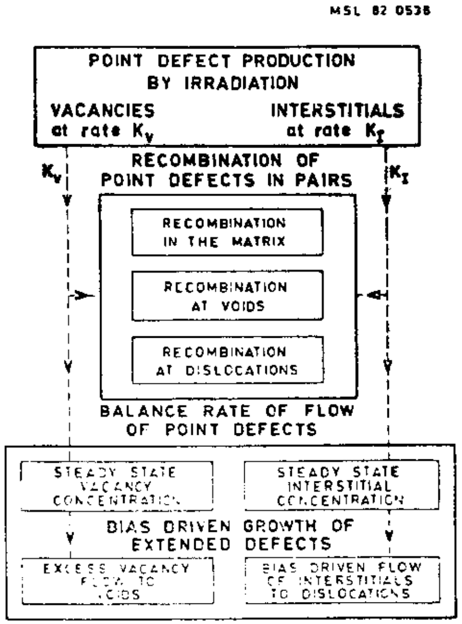

FIGURE 1 Distribution of the irradiation-produced point defects. The recombination in the matrix and at extended defect sinks results in their annihilation in pairs, while the remaining point defects contribute to a build-up of a steady-state concentration. In the presence of a biased sink point defects flow to vacancy or interstitial type sinks resulting in the observed phenomena of void growth.

Compared to void formation in metals only a qualitative picture is available[24] for the formation of voids in CaF_2. The 100 keV electron beam energy used is insufficient to directly displace either calcium or fluorine atoms. It has therefore been proposed[24] that the vacancies (or *F*-centres) are formed by non-radiative transfer of energy from an excited state into ionic motion along close packed fluorine ⟨100⟩ rows. In this case the damage or Frenkel pair defect production is confined to the fluorine sublattice only. To account for void growth, a bias arising from the behavioural difference between vacancies and fluorine interstitials has been suggested,[24,25] the latter going preferentially to form gas bubbles while the former to voids. Because of the binary nature of the compound and selective removal of fluorine into bubbles, calcium metal crystallites are expected to be formed. These crystallites are coherent with the CaF_2 matrix and are in fact the anion voids which are observed.[25] There are, therefore, significant differences both in the point defect production and the microstructure which develops in this case as compared to voids in metals.

The physical processes involved in the formation of bubbles (random distribution) are different from those in voids. Bubble growth requires the aggregation of gas atoms, and to accommodate them vacancies are normally required and are either produced thermally or by irradiation.[23,26] The temperatures for this process must be sufficiently high so that the vacancies are mobile. For this reason, in some metals helium goes into solution in the matrix both interstitially and substitutionally[27] and precipitates into bubbles at higher temperatures.[28] However, bubble formation has also been observed at room temperatures in metals like Cu, Ni and stainless steel where vacancy mobility is known to be very low.[30] In these cases either radiation-induced vacancy migration[31] or some other mechanism like the interstitial loop punching[32] due to overpressurized bubbles occurs. Unlike the case of voids the role of the irradiation is mainly to implant the desired concentration of gaseous ions, and the growth of bubbles does not require any concept like a bias or a biased sink. However, such an implantation is always accompanied by the production of vacancies and self-interstitials and the damage rates are high[33] ($\sim 10^{-3}$ dpa sec) and this influences the process of bubble growth.[34]

At first it would be natural to think that the basic mechanism for the growth of voids and the bubbles should also be linked with the process of ordering. *A priori* this connection is difficult to foresee, though it has been suggested by Chadderton *et al.*[25] that the behavioural difference of the vacancy and the interstitial which leads to random void arrays should also be responsible for the formation of the superlattices. The physical processes involved are still a matter of debate and it has not been possible to resolve these from the available experimental observations. Broadly, four stages have been suggested[8] for void ordering. (1) The initial formation of randomly distributed small voids, (2) the growth of large voids at the expense of smaller voids, (3) the appearance of small local regions where voids start having spatially ordered correlations, and (4) the spread of these regions to adjacent areas. In the case of bubble lattice, in addition to these four stages a fifth stage has been observed where (5) the small bubbles are interconnected forming pipe-like passages within the implanted layer.[33]

It is convenient to group the experimental results into four broad categories;

I Void lattices formed by neutrons and charged-particles in metals and alloys.

II Ordering of voids by electrons in stainless steel containing nitrogen.

III Bubble lattice formed by light gaseous ions in metals and alloys.

IV Void lattices by electron irradiation in alkali earth halides.

In each of these four categories, the irradiation conditions for which the ordering occurs are different. Despite this, the general features of the superlattice which emerges are remarkably similar. The first observation of void ordering in metals was by Evans[35,36] in 1971 in Mo using nitrogen ions. This was followed by similar observations using neutrons or ion irradiations in metals like Mo[35–42], Nb[38,44–47], Ta[38], W[42,48], Cb[37,49], Mg[29], Ni[49,50], Al[51] and alloys Mo–5%Ti[35,52], Nb–1%Zr[44,47], TZM[30] and Ni–2%Al.[43] In these experiments, which are clubbed together as Group I, neutrons or charged particles have been employed at elevated temperatures of about 0.3 T_m to induce ordering. Also in these cases, ordering has not been produced by electrons though they are very effective in forming voids. The only case of ordering in metals induced by electrons (Group II) has been reported by Fischer and Williams[53] for stainless steel. In this experiment the presence of a high concentration of nitrogen in the sample was found to be an important prerequisite. On the other hand, in Group III the bubble-lattices are formed generally at room temperatures. Unlike void-lattices in metals which form more readily in bcc than fcc metals, these have been observed[8,30,35,54] in fcc Cu, Ni and stainless steel, but have been formed also in bcc[55,56] Mo and hcp[33] Ti. Finally, in Group IV are the non-metallic compounds[10,24,25] like CaF_2 and SrF_2. These also involve room temperature irradiation using an electron beam. The irradiation conditions and the parameters which are involved in the ordering process are discussed below for these experiments.

2.2 *Experimental Observations on Void Ordering in Metals—Group I*

2.2.1 *Relation between void lattice and host lattice symmetry* The void lattice symmetry in bcc metals Mo, Nb, Ta, W, Cb and fcc metals Al, Ni is the same as that of the host matrix. The crystallographic orientation has also been found to coincide with that of the host matrix.[36] There have been no observed exceptions to this rule in metals (though in compounds like CaF_2 a simple cubic lattice is observed presumably related to the fluorine atom sublattice though CaF_2 has a fcc type structure[25]). This, therefore, is a fundamental property and is not influenced by impurities or irradiation conditions. The superlattice forms more easily in bcc metals than in fcc metals,[50,51] and partial ordering has been observed in hcp Mg[29] (a bubble lattice forms[33] in hcp Ti). The perfection of the superlattice depends on temperature and is best at temperature slightly less than the peak swelling value. Deviations by about 10% from perfect lattice sites, edge dislocations[52] and multiple site occupancy and vacant sites[38] are often observed. The superlattice in fcc metals is less perfect than in bcc metals.

2.2.2 *Role of radiation environment* Tables I, II and III list the metals and the nature of the irradiations which have been used to induce ordering. Any special condition like impurity gases which were found necessary are also mentioned in the last column. Several interesting features emerge. Electrons which are very effective in producing voids in metals are not effective in producing void lattices. From the tables we see that there are only two reported observations of ordering by electrons in stainless steel[53] and CaF_2.[10] In the case of stainless steel a high concentration of nitrogen atoms was found to be essential for ordering, while in CaF_2 gaseous fluorine atoms are produced. The resistance to void ordering by electrons in a large number of metals suggests that the nature of the radiation influences the ability of the voids to order. One of the well known differences between neutron or heavy ion irradiation, and electron irradiation, is that in the former cascades are formed which collapse to give vacancy loops. The influence of the radiation may indirectly arise from the extended defect structures produced and its coupling with point defects.[57] It is interesting to observe that in all cases where the radiation does not produce cascade damage the presence of gas atoms is a prerequisite for ordering. This suggests that there may be different factors involved which influence the ordering kinetics.

2.2.3 *Dose rate effect* Experimental results show that irradiation dose rate is not an important parameter for ordering. Several elements and alloys like Cb[37], Nb[44–47], Nb–1% Zr[38,44,47], Mo[35–39] and TZM[38] (Mo–5% Ti–0.1% Zr) have been irradiated both by neutrons[37–39,45] at approximately 10^{-6} dpa/sec and heavy ions[33–37,44,46,47,58] (see Table I) in the range 10^{-3} to 10^{-2} dpa/sec. In all these cases void ordering with generally similar features has been observed. However, for a direct comparison of the results at different dose rates care has to be taken for the dose rate dependent shift in the peak swelling temperatures and the differences in the concentration of voids and other microstructural features. A detailed comparison has been made by Eyre and Evans[39] for Mo irradiated at 650°C by neutrons at a dose rate of 10^{-6} dpa/sec and also irradiated at 870°C by 2 MeV nitrogen ions at a dose rate of 7×10^{-3} dpa/sec. For these irradiations the superlattice spacing was 340 Å and 220 Å and the average void radius 19 Å and 20 Å for neutrons and ions respectively. Considering that the cyclotron irradiation temperature of 870°C is equivalent to a reactor irradiation temperature of 680°C the superlattice parameters for vastly different dose rates are in reasonable agreement.

2.2.4 *Dose dependence* It is observed that voids (and bubbles) initially form randomly and subsequently start ordering.[8] The dose at which the ordering commences is difficult to determine and most experiments, therefore, report the final dose at which the ordered structure is observed. However, in some cases there appears to be a threshold dose before the onset of ordering. In the case of ion-irradiated Ni this threshold is reported[49,50] to be in the range of 350 or 400 dpa. Similarly, a high critical dose of 40 to 80 dpa is required for Al.[51] There are no reported values for critical dose for bcc refractory metals but comparatively the value is lower. Kulcinski *et al.*[39] have irradiated Nb, Mo and TZM to 5 dpa in the temperature range 600 to 1000°C using 5 MeV Ni ions. Ordering was only observed in Nb at 800°C, indicating that the critical dose is less than 5 dpa, a result corroborated by Loomis *et al.*[44] In the case of other elements the critical dose is higher but less than 36 dpa since ordering has been observed at this value. Loomis *et al.*[44,47] observe that no ordering occurs in Nb containing less than 60 ppm of oxygen and in Nb–1% Zr containing less than 400 ppm oxygen regardless of the irradiation temperature (650–1010°C) or irradiation dose 2–140 dpa, but at higher oxygen concentrations ordering has been observed. There seems to be no dependence of the critical dose on the oxygen concentration but a threshold oxygen concentration is required to induce ordering. Also the reported dose values where ordering has been observed by heavy ion irradiation is much higher than by neutron irradiation (with a few exceptions like Nb). These experimental results (see Table I) suggest that the critical dose may not be an explicit parameter for the onset of ordering but may be implicitly related

TABLE I

Compilation of the irradiation conditions and void lattice parameters in elements and alloys—Group I

Material	Projectile	Energy MeV	Temperature °C	Dose dpa	Spacing D Å	Diameter ($2r_v$) Å	Remarks	References
Ta	*n*	>0.1	585	20	205	61		38
W	*n*	>0.1	550	15	195	30		42
	n	>0.1	880	15	250	40		48
Mo	*n*	>0.1	585	36	265	64		38
	n	>0.1	790	36	328	72		38
	n	>0.1	650	30–60	340	38		39
	n	>0.1	600		280	54		61
			715		328	57		
			880		370	60		
			900		358	58		
			920		390	56		
	N	2	870	100	220	40	Influenced by gaseous impurities.	40
	Ta	7.5	900	130	230	60	See Ref. 72	37
Cb	Ta	7.5	800	140	340	125		37
	Ta	7.5	800	290	380	110		37
	Ta	7.5	900	300	750	250		37
Nb	*n*	>0.1	790	34	665	186		38
	n	>0.1	800		685			45
	Ni	5	800	5	350	45		49
	Ni/V	3.2	650	30	100	20	Threshold O_2 60–400 ppm required—see **Ref.** for complete data and Figures. 2 and 3	44, 47
			805	5	100	20		
			805	10	240	50		
			805	40-140	360	135		
			825	30	450	200		
			925	20	550	225		
			925	40-140	620	250		
			1010	30	1450	750		
Ni	Ni	5	525	360	620	250	No effect of 3 ppm He	49
	Sc	6	525	400	660	150	O + N + H 200 ppm	50, 49
Al	Al	0.4	50	40	600	100	He doping improved alignment	51
			75	80	600-800	140		
Mg	*n*	>0.1	55	3-6			Imperfect unidimensional lattice	29
Ni-2% Al	N	0.4	500	10	887	173	Possible formation of Al depleted regions around voids	43
				20	499	136		
				40	455	110		
				70	465	139		
Ni-4% Al	N	0.4	500	10	985	111		
				20	513	131		
				40	485	117		
				70	452	119		
Ni-6% Al	N	0.4	500	10	1463	101		
				20	502	107		
				40	360	63		
				70	492	116		
Ni-8% Al	N	0.4	500	10	1543	106		
				20	570	105		
				40	453	95		
				70	443	100		
Mo-5% Ti	*n*	>0.1	585	36	215	69		38
	n	>0.1	790	36	315	72		38
	n	>0.1	580		220	40		52
Nb-1% Zr	Ni/V	32	650–1010	2-140	100–1450	20–750	See table for Nb Ref. 44, 47 Ordering only if O_2>4000 ppm	44, 47
TZM	N	2	870	400	220	60		36
	n	>0.1	600		276	52		61
			715		300	52		
			880		370	52		
			900		387	59		
			920		365	51		

TABLE II

Compilation of irradiation conditions and bubble lattice parameters in metals—Group III

Material	Gas/ Projectile	Energy MeV	Temperature °C	Dose ions/cm²	Spacing *D* Å	Diameter Å	Remarks	References
Mo	He	36	RT*	1×10^{17}	37			55, 56
		36	300	2×10^{17}	34			
		36	400	2×10^{17}	50			
		36	500	2×10^{17}	36	~24		
		36	700	2×10^{17}	35			
		25	250	4.5×10^{17}	32			
		40	300	2×10^{17}	35			
		40	400	5×10^{17}	36			
		60	400	2×10^{17}	45			
		40	500	5×10^{17}	38			
Mo	Ne	100	550	1×10^{17}	36		**No details available**	56
Cu	He	30	RT	4×10^{17}	77	20		9, 30, 33
	H	16	RT	1.3×10^{19}			Lattice parameters not well defined	65
Ni	He	30	RT	4×10^{17}	66	20		9, 30, 33
AISI 321 Steel	He	30	RT	4×10^{17}	64	20		9, 30, 33
316 SS	He	30	RT	4×10^{17}	65	20		33
Ti	He	30	RT	1.5×10^{18}	90	30	Typical estimates 50% more than Cu	33

*RT—room temperature.

TABLE III

Compilation of irradiation conditions for ordering induced by electrons in stainless steel and alkali earth compounds—Groups II and IV

Material	Electron beam energy	Temperature C	Dose dpa	Spacing *D* Å	Diameter Å	References
20/25 stainless steel	2 MeV	500	20	250	80	53
CaF_2	100 keV	RT*		192–283	~20	10, 25
SrF_2	100 keV	RT		—	—	25

*RT—room temperature.

to the development of some appropriate microstructural or other conditions which determine the onset of ordering.

The dose dependence of the superlattice spacing has been studied[44–47] for Nb with 5200 ppm oxygen and Nb–1% Zr with 3500 ppm oxygen. The results are reproduced in Figure 2. At 805°C the void lattice parameter increases from about 100 Å to 375 Å and void radius from 10 Å to 67 Å between 2 and 30 dpa respectively. After 30 dpa the superlattice parameters reach a saturation and therefore are independent of dose. Similar features have been reported at a higher temperature, 925°C, and the void spacing and diameter increase with temperature. The saturation of the superlattice parameters as a function of dose is an important characteristic of the ordered structure which is clearly brought out by these results.

2.2.5 *Effect of alloying components and gas atoms*

It has now been established that small quantities of alloying elements influence the swelling characteristics of metals.[59,60] It is difficult to isolate these effects from those which may specifically be involved in the ordering of voids. Wiffin[38] has studied the effect of alloying in elements and alloys namely, Mo, Mo–0.5% Ti, Nb, and Nb–1% Zr after neutron irradiation. There was no significant difference in the void superlattice in Mo and its alloy though the void concentration was higher in

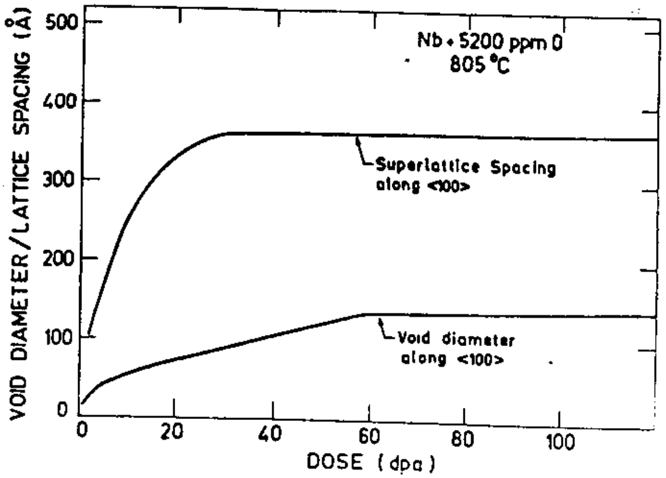

FIGURE 2 Void lattice spacing and diameter as a function of dose in Nb with oxygen impurity (from Ref. 44). Observe the slight dose dependence in the D/r_s ratio at low doses.

the latter. Ordering has been observed in Nb but not its alloy, though ordered void lattice has been observed by others both by neutron and ion irradiation in Nb-1% Zr. Similar results have also been reported for Mo and TZM under neutron irradiation.[61] A detailed study of the effect of alloying in Ni-x% Al (x = 0, 10) has been made by Chen and Ardell[43] at 500°C using 400 keV nitrogen ions (Table I). They find that for 2% Al alloy the best results are obtained while for higher concentration the degree of alignment becomes poor and no ordering is observed in pure Ni till 70 dpa. Void lattice parameters are only weekly sensitive to alloy composition.

On the other hand, specific results have been reported on the effect of implanted gases on superlattice formation by Loomis *et al.*[44,47] They have studied the influence of oxygen on Nb and Nb–1% Zr irradiated by 3.2 MeV Ni^+ and V^+ ions. They find that a threshold oxygen concentration is required to induce ordering. This threshold value is reported to be between 60 and 400 ppm in Nb and between 400 and 2700 ppm in Nb–1% Zr, depending on temperature (650–1010°C). It is perhaps significant that the low oxygen concentration completely suppresses void superlattice formation rather than influencing the critical dose for the onset of ordering. Once the oxygen threshold concentration is available the superlattice parameters are *independent* of the oxygen concentration. The presence of a high concentration of nitrogen gas has also been reported to be a prerequisite for ordering in stainless steel by electrons.[53] In Ni, however, no such threshold effects due to He have been observed[49] though the void density increases because of the higher number of nucleation sites available.

2.2.6 *Temperature dependence of void lattice parameters and stability* Very few systematic investigations on the temperature dependence of the void lattice parameters have been reported in the literature. Wherever measurements have been made at two different irradiation temperatures results indicate that both the void spacing and the void diameter increase with temperature. A detailed study has been done by Loomis *et al.*[44,47] in Nb and Nb–1% Zr in the temperature range 650 to 1010°C. The results are reproduced in Figure 3 and show a strong temperature dependence. The average void radius r_s increases from about 10 Å to 375 Å and the lattice spacing D from 100 Å to 1450 Å over the temperature range. A small peak is observed at 825°C whose origin is not clear but is attributed to the diffusion of the oxygen impurity to the void surface. The temperature dependence is not linear and rises rather sharply after 900°C. In the case of random void arrays, it has also been observed that the void density decreases sharply and average void diameter increases with increasing temperature.[62] Though an exact correlation cannot be established, the temperature dependence of the void lattice parameters may be related to the kinetics of void formation rather than to any considerations based on the stability of the void lattice. A similar observation has also been made by Moteff *et al.*[42] The ratio of the void spacing to average void radius r_s has been observed to be nearly independent of temperature and irradiation conditions. It has, therefore, been regarded as an important parameter which depends mainly on the material properties.[16] However, a weak temperature dependence has been observed[44] which cannot be explained completely on the basis of the temperature variation of material properties like elastic anisotropy of the host matrix.[48] Figure 4 shows the observed values of D and r_s for various metals and the slope gives the ratio D/r_s which varies from 4 to 15 in most metals.

Though the void lattice forms over a wide range of temperatures, deviations are observed from the perfect lattice sites and the perfection is best at

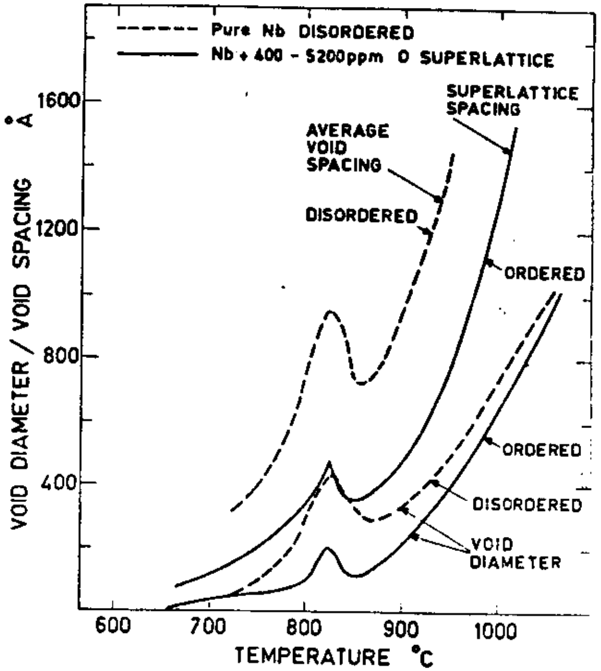

FIGURE 3 Void lattice spacing and diameter for ordered voids in Nb containing oxygen (from Ref. 44) and average void spacing and diameter for a disordered distribution in pure Nb (from Ref. 62) as a function of temperature.

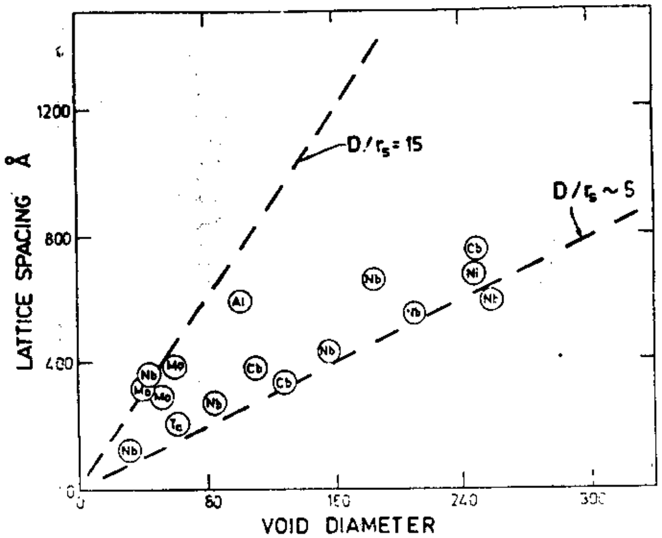

FIGURE 4 Void lattice spacing and diameter for various elements. Different values for the same element reflect the dependence on irradiation conditions like dose and temperature. The D/r_s ratio lies between 15 and 5 approximately. For a more complete list and references see Tables I–III.

temperatures just below the peak swelling value. There is no clear evidence on the factors which contribute to this perfection. However, if the voids had the ability to move and if elastic interactions are involved, it should be possible to improve the alignment by post-irradiation annealing at high temperatures. This is not borne out by experiments[63] and suggests that dynamic irradiation conditions are involved in inducing the ordering. Evans *et al.*,[64] however, have reported void formation in Mo by annealing at 900°C after neutron irradiation at a low temperature (60°C). They observe that in some cases where a high density of voids is formed, they are partially aligned into an imperfect lattice array with the same symmetry (bcc) and orientation as the host matrix. The conditions for which this ordering occurs is not understood, but the presence of gaseous impurities may play an important role.[64]

Another important property of the void lattice is its stability. High-temperature annealing shows that, compared to isolated voids, the void lattice is stable till much higher temperatures. In Mo, for example, an isolated void shrinks at 1100°C but a void lattice is stable till nearly 1500°C.[8]

2.3 *Ordering in Electron Irradiated Stainless Steel—Group II*

The observations by Fisher and Williams[53] are the only reported results of void ordering in metals by electrons. The ordering was observed in 20/25 stainless steel containing Ti which after nitriding exists as TiN phase and is not expected to influence the ordering process. However, the presence of a high concentration of nitrogen in the sample (~0.5 wt.%) was found to be an essential prerequisite and leads to a higher void density as compared to the untreated steel. A saturation in the void radius and spacing was observed at 40 Å and 250 Å respectively for a dose of 20 dpa. An important observation is that the ordering occurred at relatively low temperatures ~500°C, which are reported to be well below the peak swelling value. This fact may be of significance since it implies low vacancy mobility, a feature which is shared with the observed bubble lattices where the ordering occurs at room temperatures[9] (see Table III).

2.4 *Bubble Superlattice Formation in Metals—Group III*

Helium bubble superlattice was first observed in bcc Mo by Sass and Eyre[55] and Mazey *et al.*[56] They have also mentioned the formation of a neon-lattice[56] in Mo. These results have been followed by a series of papers by Johnson and Mazey,[9,30,33] where they have reported helium bubble lattice in fcc metals Cu, Ni, stainless steel and in hcp Ti.[33] They have also observed[65] an ordered hydrogen gas bubble-lattice in Cu. The irradiation conditions and the observed bubble lattice parameters are given in Table II. There is a remarkable qualitative similarity between the bubble lattice and the void lattice. In all the reported observation on bubble lattice formation the crystallographic symmetry and its orientation is the same as that of the host matrix. The ratio of the bubble lattice spacing to bubble radius is also in the same range as that for void lattices. The general observations regarding the stages of ordering are also similar to those for voids, starting initially with a disordered distribution which gradually orders in local regions and this order spreads to other parts. A fifth stage, which has been reported when the ordering is nearly over, is an interconnection between strings of bubbles through pipe-like channels.[33]

Amongst the significant differences between the void lattice and the bubble lattice are the absolute values of the lattice parameters. The average bubble radius is typically 20 Å and the lattice constant in the range 60–80 Å which is nearly a factor of 10 smaller than for void lattices. Most of the irradiation studies for bubble lattices have been done at room temperatures in contrast to higher temperatures required for void formation. This temperature in the case of all the metals studied (Table II) is too low for any significant vacancy migration, though irradiation enhanced diffusion cannot be ruled out.[31] This introduces an important difference with the case of voids where vacancy migration is essential for void formation. In the case of bubble lattice, irradiation results in the temperature range 20°C to 700°C have been reported for Mo by Mazey *et al.*[56] Bubble lattices have been observed at all these temperatures but not at 750°C. In contrast to void lattice results of Loomis *et al.*[44] for Nb where they observe a strong temperature dependence in both the average void radius and void spacing (see Figure 3) the bubble lattice parameters are essentially temperature independent as can be seen from Table II.

The formation of a bubble lattice does not appear to be a specific property of the helium gas; such ordered lattices have been reported for H,[65] He[9,30,33,55,56] and Ne[56] gases though in the case of H the lattice ordering is not as well defined as compared to He.[65] The hydrogen bubbles exhibit a wide range of sizes and are not spherically well defined, the lattice parameter also appears to vary from place to place. The dose required are typically 4×10^{17} He^+/cm^2 for fcc metals like Cu, Ni and stainless steel, 1.5×10^{18} He^+/cm^2 for hcp Ti for which the observed bubble size and spacing is a factor of 2 more than for fcc metals.[33] These doses are less than the critical dose for blistering. In the case of hydrogen gas-bubble lattice in Cu a much higher dose of $\sim 1.3 \times 10^{19}$ H^+/cm^2 was required.[65] Estimates of the implanted gas show that the helium bubbles may be overpressurized by a factor of ~20 if all the helium gas implanted is in bubbles.[30] However the overpressurization may be lower (~5) with some of the gas being in solution in the matrix. Johnson and Mazey[31] have also reported very interesting results on electron irradiation subsequent to bubble lattice formation. By electrons only damage effects in the form of vacancies and interstitials are produced. They found that in Cu the average bubble radius increased from 10 Å to 14 Å and the spacing from 70 Å to 90 Å. This suggests that a considerable amount of He must be present in solution presumably as a complex He^6V with vacancies.[34] Also the experiment shows that damage effects influence the process of bubble formation.[66] The damage rates in low energy He irradiation experiments are quite large being of the order of 10^{-3} dpa/sec. The thermal stability of the bubble lattice is also good and it survives temperature as high as 0.4 T_m after which they grow coalesce and produce blisters.[30]

2.5 *Ordering Effects in Compounds—Group IV*

The experimental observations on ordering of voids in compounds like CaF_2 and SrF_2 and the resistance to ordering in other alkali earth and alkali halides have been reviewed by Chadderton *et al.*[25] They have also discussed the implications of these observations to void ordering in metals and the main results are summarized here. Room temperature irradiation has been done using a 100 keV electron beam on natural fluorite (CaF_2).[10] The energy is insufficient to directly displace Ca or F atoms and a mechanism based on a non-radiative energy transfer via electrons to the lattice is visualized.[24,25] This produces a linear replacement sequence along the ⟨100⟩ direction which involves only the anions sublattice producing a vacancy and fluorine interstitial. Since the observations are made under normal operating conditions of electron microscopy some details on the dynamics of the ordering are available. It is reported[10] that a dark contrast double loop structure is first seen which grows and coalesces. Simultaneously a speckled structure consisting of small electron transparent zones appears which grows and performs a Brownian-like motion. This eventually develops into three-dimensional stable static array, and the loop structure disappears. Earlier this ordering was mistaken to be colour centre aggregates,[67,68] but more detailed studies have confirmed them to be voids. The loop contrast structures may be bubbles containing fluorine gas.[10] Due to the binary nature of the compound calcium crystallites are expected to be formed and these constitute the observed voids since fcc Ca crystallites are coherent with CaF_2 structure. A relatively less perfect void lattice has been also observed in SrF_2 but the voids show a strain contrast because of the slight difference in the lattice parameters of Sr crystallites and SrF_2. No ordering is observed in BaF_2 and the alkali halides due to the incoherent precipitation of the metal ion which produces a large strain and probably impedes the motion of voids.[24]

The most striking feature is that the superlattice in the fluorite is simple cubic and seems to be only related to the fluorite sublattice though the fluorite structure is fcc.[10] The observed lattice spacing at room temperature is between 190 and 280 Å with the ratio of the void spacing to void radius ranging between 4.5 to 7.5[23] and is of the same order as void lattices in metals (Table III).

3 ORDERING AS A NON-EQUILIBRIUM PHASE TRANSITION

Theoretical models have been proposed mainly to understand the ordering of voids in metals (Group I). At present only qualitative extensions of these models have been discussed to understand void and bubble lattices in other systems and these will be considered in Section 3.2. Here the theoretical models which view void ordering in metals as a non-equilibrium self-organization process are described.

3.1 *Microstructure Induced Instability Model*

3.1.1 *Soft mode instability, fluctuations and bifurcation* The microstructure-induced instability model has been proposed by Krishan.[57,69] A qualitative picture for this model is developed first and is followed by a more detailed discussion. During irradiation of a metal, point defects and extended defects like voids, dislocation loops, etc., are produced. The extended defects are randomly distributed at discrete spatial positions and act as sinks for the point defects. Generally the interest is not in the detailed evolution of each individual extended defect but rather in their collective behaviour.[70] It is convenient, therefore, to replace the real system by an effective homogeneous lossy medium.[71] In the lossy medium each type of extended defect retains its identity but not its discrete character, since it is assumed to be homogeneously distributed throughout the medium in a way that it has precisely the same properties as a sink for point defects as in the real system. This requires a self-consistent modelling of the sink strength for each sink type (like void, dislocation loop, etc.). This approximation is in the same spirit as the meanfield treatment employed in a number of physical problems like those encountered in magnetism and atomic physics. The theoretical justification for this procedure has been discussed by Brailsford,[73] and recently reviewed by Brailsford and Bullough.[22]

In the lossy medium picture the evolution of the system in the presence of irradiation is described in terms of the point defect concentrations C_V and C_I (suffix V for vacancies and I for interstitials) and sink parameters ρ_s, ρ_v, ρ_i and ρ_d (suffixes s, v, i and d for voids, vacancy loops, interstitial loops and dislocations respectively).[20] These variables characterize the system and are functions of time only and not of space (the spatial dependence is lost because the discrete nature of the extended defects is replaced by homogeneously distributed sinks in the medium). The individual sink terms ρ are related to the concentration N of each extended defect type and to a size parameters such as the average radius. These relations are obtained self-consistently by solving the diffusion equation[70] but for the present discussion it is sufficient to consider the first order expressions given by [20] $\rho_s = 4\pi N_s r_s$,

$\rho_v = 2\pi N_v r_v$, $\rho_i = 2\pi N_i r_i$ and ρ_d, the network dislocation density. The time dependence of ρ can arise due to the changes in N, r or both. Normally, at high doses, the void and the interstitial loop concentration N tend to saturate and the radius r increases with dose. On the other hand in the case of the vacancy loops, due to their athermal formation, the concentration N_v changes with dose.

The homogeneous lossy medium picture provides a good mathematical description of the *average* behaviour of the real physical system. However, in this process the information about the spatial distribution of the extended defects is lost. How do we then understand the spatial ordering of the extended defects in the framework of this theory? A characteristic of any spatially ordered structure is a wavelength λ which describes the periodicity of the system. This wavelength λ arises due to some scale length which is related to the physical processes in the system. The distribution of the voids is initially random and ordering commences only at higher doses. A characteristic of the random distribution is that no specific wavelength can be associated with it, and this feature is retained in the picture of the homogeneous lossy medium. If a specific wavelength has to emerge with dose the system must *deviate* from the homogeneous state and show spatial variations.

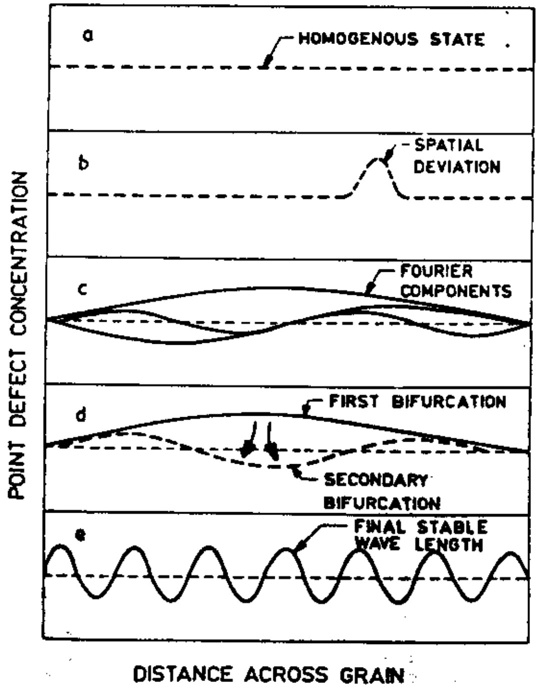

FIGURE 5 Schematic representation of the behaviour of the point defect concentration during an instability. (a) Homogeneous steady state; (b) spatial fluctuation in concentration; (c) spatial fluctuation decomposed into different modes; (d) first bifurcation, and the bold arrows show how it can further bifurcate; (e) a periodic variation in the concentration due to secondary bifurcations leading to void ordering.

To visualize why a system tends to deviate, consider the irradiation processes in a grain of length d, which will be considered to be modelled as a lossy medium. Figure 5(a) shows the homogeneous concentration C (C_V or C_I) of the point defects at any instant of time t during the irradiation. Let a small inhomogeneity develop so that the concentration C changes to $C+\delta C$. Since the inhomogeneity is spatial, the deviation $\delta C(x, t)$ will be a function of x and t as shown in Figure 5(b). We are interested in examining how $\delta C(x, t)$ will evolve in time. Three physical situations can be considered. In the first case the point defects are mobile and the inhomogeneity introduces a gradient in the point defect concentration. By Fick's law, the point defects will diffuse to regions of lower concentration at a rate proportional to $D\nabla^2\delta C(x, t)$, where D is the point defect diffusion constant. The deviation $\delta C(x, t)$ therefore decays, the inhomogeneity cannot be sustained and the system approaches the original homogeneous state. The sink nature of the lossy medium has not been incorporated so far. In the second case the homogeneously distributed sinks are *not* influenced by the deviation $\delta C(x, t)$ in the point defect concentration and only provide an additional mechanism for the loss of point defects. The deviation $\delta C(x, t)$ in this case will again decay to zero[67] but the characteristic time constant τ in which it decays would be different because of the additional loss of the point defects to sinks. In the third case the coupling of the point defects with sinks is considered. Due to this coupling the local sink strengths at x will also change by $\delta\rho(x, t)$ due to the deviation $\delta C(x, t)$ and the inhomogeneity in the point defects will be coupled to the inhomogeneity in the sinks. Further evolution of $\delta C(x, t)$ will depend not only on the gradient in the point defect concentration, but also on the *local* values of the sink strengths. Depending on the physical nature of the coupling between the point defects and the different types of sinks, such an inhomogeneity can result in a relative increase in the local point defect concentration at x so that the time constant τ is increased. In particular τ can become infinite which implies that the inhomogeneity will persist and the system deviates from the homogeneous state. The coupling between the microstructure and the point defects is an essential feature of Krishan's model.[69] However, whether τ increases or decreases depends on how $\delta\rho(x, t)$ itself evolves and therefore is related to the *specific* types of microstructural defects which are present in the system and the dynamic equations they obey.

Another way to view this physical situation[16] is to resolve the deviation $\delta C(x, t)$ into Fourier components with coefficients a_m;

$$\delta c(x, t) = \sum_m a_m \exp(\omega_m t) \sin \frac{m\pi x}{d} \tag{1}$$

This is shown schematically in Figure 5(c) where $\delta C(x, t)$ is a superposition of a number of waves having wavelengths λ_m; $\lambda_m = d/2m$, $m = 1, 2, 3 \ldots$. The ω_m's are the inverse of the characteristic time constants $\tau_m = \omega_m^{-1}$ associated with each wavelength λ_m and are referred to as the eigenfrequencies. It may be observed from Eq. (1) that if $\omega_m < 0$ for allowed values of m, then $\delta C(x, t)$ goes to zero. Physically this can be interpreted to imply that if $\omega_m < 0$ for all m values, no wavelength λ_m can be stable and any inhomogeneity will decay with the system approaching the homogeneous state. This reasserts the original statement that the homogeneous state cannot be characterized by any wavelength. The frequencies depend on the rate constants of the reactions between the point defects and the sinks and their quasi-stationary concentration and sink strength respectively. Therefore, *ω_m's are not explicit functions of time* and can be regarded to be functions of some other parameter like the average sink strength which itself may slowly increase with time. This parameter is referred to as the control parameter.[17] For an appropriate coupling of the point defects with the microstructural variables, as the control parameter approaches a critical value, one of the eigenfrequencies ω_m becomes zero. This implies that the decay time constant $\tau_m = \omega_m^{-1}$ becomes infinite and therefore the wavelength λ_m corresponding to this mode will be sustained in the system and as a result of this it bifurcates from the homogeneous state. This in some respects is analogous to structural phase transitions[74] where one of the vibrational frequencies becomes zero at a critical temperature and the system undergoes a structural change of phase. This frequency is related to a specific vibrational mode of the solid and is referred to as the soft mode[75] when the vibrational frequency becomes zero. In the present case δC was defined as the deviation in the point defect concentration from the average steady state value. More appropriately it should be a deviation involving a linear combination of the system

variables which would correspond to a specific mode of the coupled nonlinear system.

The specific wavelength which emerges depends on the mode which becomes soft and this depends on the functional relationship of ω_m on the control parameter.[76] In many systems (as is also the case with the void lattice) it is the longest wavelength corresponding to $m=1$ which emerges first,[16] this is the first bifurcation, and is shown in Figure 5(d). However, this mode itself may develop a further instability and bifurcate again by a cascade process[77] till finally it stabilizes at some value m. The evolution of the system during this multiple cascading phase is extremely complex since it involves a stability analysis of a state of a system which shows both time and spatial dependence.[78] A detailed description during this stage of evolution has not been attempted. Despite these limitations the conditions for which the first bifurcation occurs provide an understanding of the kinetic processes responsible for the ordering. Also some estimates can be made regarding the spatial correlations which will eventually develop, and this gives an estimate of the wavelength which is likely to emerge (Figure 5(e)).

The above discussion has been made with reference to a lossy medium and therefore must be related to the physical processes in the real system. The presence of an instability in the lossy medium implies that the real system will have a *tendency* to develop into a spatially dependent structure. However, the bifurcation to the new state is driven by the presence of fluctuations in the system.[79] There are various factors which contribute to these fluctuations like the intermediate reactions which the point defects undergo with impurities,[80] fluctuations due to cascade formation[81] or even chemical fluctuations involving concentration variables.[82,83] Due to the presence of these fluctuations the extended defect structure variables can either deviate to a new trajectory in phase space (of the system variables) the system still remaining *homogeneous* or it can start showing spatial dependence. In the first case the fluctuations are purely temporal in nature while in the second case they are spatial as well. The case of temporal fluctuations has been studied in detail,[80] however, a rather simple idealized picture can be adopted to understand their influence. At temperatures where thermal emission of vacancies from extended defects is not important, the extended defect like a void can be looked upon as a "Brownian particle" in a fluid of point defects. The fluctuations in the point defect concentration influence the flow of point defects into the voids. It has been shown[80,84] that in the regime where point defect recombination is a dominant mechanism of point defect loss, the dynamic equations are only marginally stable[84] and one of the eigenfrequencies becomes soft. For these conditions the point defect concentration deviates linearly in time from the average value, and this therefore influences the growth kinetics of voids which show similar deviations from the average growth rate predicted by the rate theory.[80] Though this calculation has not been done for the soft mode related to the spatial instability, a somewhat similar picture can be adopted. Spatial fluctuations are present all the time but they do not normally affect the system because they decay in time since the homogeneous state is stable. However in the presence of an instability these fluctuations grow with time and because of their spatial character will result in a Brownian-like motion of the voids and other extended defects. It is possible that in the observation of Chadderton *et al.*[10] the motion of voids seen by them by electron microscopy during ordering arises due to this reason. This motion, however, will be influenced by the *interactions between the extended defects and any anisotropy in the point defect diffusion*. The system will therefore evolve under all these influences to form a new spatially ordered structure. The process of void ordering must therefore be viewed in its totality; the non-equilibrium instability gives the kinetic conditions for the onset of ordering while the anisotropy and the lattice nature of the host matrix influence and determine the final structure which emerges. The microstructural instability model must, therefore, not be viewed as an alternative to other models[63,85] but must be considered in conjunction with them to gain a complete picture. Figure 6 summarizes the main features of the instability discussed in this section.

3.1.2 *Mathematical formalism* The most important aspect of the microstructural model[57,69] is the coupling between the point defect concentrations and the microstructural sink densities and these are defined by the Bullough–Eyre–Krishan (BEK) equations[20] used in the theory of void growth (random distribution). In the BEK model the time development of the point defect concentrations is given by

$$\frac{dC_V}{dt} = K_V - \beta_V C_V - \alpha C_V C_I + D_V \nabla^2 C_V \tag{2}$$

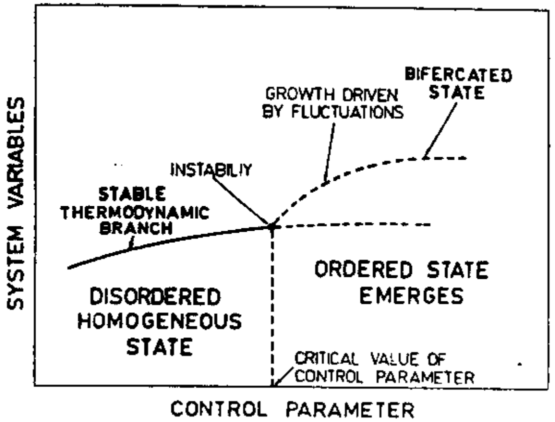

FIGURE 6 Schematic diagram showing the disorder to order transition when the control parameter reaches a critical value. The regions of the homogeneous state, instability, growth due to fluctuations, and the final emergence of the bifurcated ordered state are shown.

and

$$\frac{\mathrm{d}C_I}{\mathrm{d}t} = K_I - \beta_I C_I - \alpha C_V C_I - D_I \nabla^2 C_I \tag{3}$$

Here K's are the point defect production rates, α the recombination constant and β's are functions of the sink densities and the bias Z_I which allows for the preferential flow of the self-interstitials to dislocations. The β's are defined by

$$\beta_V = D_V(\rho_s + \rho_v - \rho_i + \rho_d) \tag{4}$$

and

$$\beta_I = D_I\rho_s + Z_I D_I(\rho_d + \rho_v + \rho_i) \tag{5}$$

The additional terms involving the Laplace operator in Eqs. (2) and (3) take into account the point defect diffusion. In the absence of these terms the rates C_V and C_I can be set equal to zero to obtain the homogeneous steady-state solutions C_{V0} and C_{I0}.[20] These solutions are also valid when the diffusion terms are added since $\nabla^2 C_{V0} = \nabla^2 C_{I0} = 0$. However, since the Eqs. (2) and (3) are nonlinear, they can therefore have other spatially dependent solutions. The nonlinearity in these equations can be ascribed to the recombination term $\alpha C_V C_I$. However, this nonlinearity does not give rise to an instability in these equations as shown by Krishan[65] and Martin[66] and additional interactions between point defects or off-diagonal diffusion coupling between them has to be included. Models on these lines have been proposed by Martin[66,67] and Imada.[68] In the microstructural model, however, the sink terms $\beta_V C_V$ and $\beta_I C_I$ are regarded as nonlinear since β_V and β_I are functions of the microstructural variables like the vacancy loop concentration N_V or void radius r_s (see Eqs. (4) and (5)) and deviations in these variables have to be considered together with those in the point defect concentrations. The factors which contribute to the instability in this model are therefore different from those in the models by Martin[66,67] and Imada.[68]

Let us consider the equations for the evolution of the microstructure. In the BEK model the interstitial loop and void concentrations are assumed to attain a steady state and the rate equation for the average radius of interstitial loops and voids is respectively given by

$$\frac{\mathrm{d}r_i}{\mathrm{d}t} = \frac{1}{b}[Z_I D_I C_I - D_V C_V + P_i(r_i)] \tag{6}$$

and

$$\frac{\mathrm{d}r_s}{\mathrm{d}t} = \frac{1}{r_s}[D_V C_V - D_I C_I - P_s(r_s)] \tag{7}$$

where b is the host lattice constant. The vacancy loop radius, however, shrinks at a rate

$$\frac{\mathrm{d}r_v}{\mathrm{d}t} = \frac{1}{b}[D_V C_V - Z_I D_I C_I - P_v(r_v)] \tag{8}$$

but because of their continuous athermal production at a rate n_v their concentration N_v changes with time and is given by

$$\frac{\mathrm{d}N_v}{\mathrm{d}t} = n_v - \frac{N_v}{r_v b}[Z_I D_I C_I - D_V C_V + P_v(r_v)] \tag{9}$$

where r_v is the average vacancy loop radius. The terms P_i, P_s and P_v are related to the thermal emission rates of vacancies. The explicit form of P's is not important for the present discussion and is given elsewhere.[18-20] An important physical fact which emerges from these equations is that only the void and the vacancy loop Eqs. (7) and (9) contain nonlinear coupling terms C_V/r_s, C_I/r_s, $N_v C_V$ and $N_v C_I$ between the microstructural variables (r_s, N_v) and the point defect concentrations C_V and C_I (The nonlinear r dependence in the thermal emission terms P does not couple with the point defect concentration. Such coupling terms contribute to the off-diagonal terms in the dynamical matrix for the deviations.) In the case of interstitial loops there are no such coupling terms and Eq. (6) is linear in the concentrations C_V and C_I. This implies that a spatial deviation in the point defect concentration does not couple in the same way with interstitial loops as with voids and vacancy loops. Also since the interstitial loop equation is linear interstitial loop production cannot cause an instability resulting in the bifurcation of the system from the homogeneous state. This difference between the interstitial loops and the vacancy loops accounts for the resistance to void ordering by electron irradiation where interstitial loops form but cascade damage and associated vacancy loop production does not occur. Experimentally dislocation loop alignment together with voids has been observed[69] and the loops identified to be vacancy type. A more detailed discussion on this is given in the next subsection.

The main arguments for the instability analysis are as follows. In the four coupled rate Eqs. (2), (3), (7) and (9) the diffusion terms $D_V\nabla^2 C_V$ and $D_I\nabla^2 C_I$ appear only for the point defect equations since the extended defects are immobile. A solution of these equations gives the average behaviour of the system.[20] We are, however, not interested in this average behaviour but in the evolution of the system if it deviates from this state. Let δC_V, δC_I, δN_v and δr_s be the deviations (functions of space and time) which can be compactly written as a column matrix with $\delta \mathbf{C}_P = \{\delta C_V, \delta C_I\}$ and $\delta \mathbf{C}_E = \{\delta N_v, \delta r_s\}$. If these deviations are small, then the further evolution can be obtained by linearizing these four equations and is given by the 4×4 matrix equation

$$\frac{\mathrm{d}}{\mathrm{d}t}\begin{pmatrix}\delta C_P\\ \delta C_E\end{pmatrix} = \left[\begin{pmatrix}A_{11} & A_{12}\\ A_{21} & A_{22}\end{pmatrix} + \begin{pmatrix}D & 0\\ 0 & 0\end{pmatrix}\nabla^2\right]\begin{pmatrix}\delta C_P\\ \delta C_E\end{pmatrix} \tag{10}$$

Here A's are 2×2 matrices which are functions of the average homogeneous point defect concentrations and the sink densities in the system and D is a diagonal matrix with elements D_V and D_I. In the above matrix equation δC_P and δC_E are arbitrary deviations which can be expressed in terms of a linear combination of suitably defined basis functions. The advantage is that any random fluctuation can be reconstructed from the basis functions. Though there is freedom in the choice of the basis functions it is convenient to take them so that they reflect the global symmetry of the system and the ordered structure which emerges. Since the above equations involve the Laplace operator ∇^2 the region over which the fluctuation appear must be defined. Consider the system to be made up of grains which can be treated to be independent with no spatial correlations between them. This assumption is justified because the grain boundaries are perfect absorbing sinks for point defect and each grain therefore behaves independently. Since the shape of the grain is not important, it will be assumed to be a cube of side d and the basis functions are represented by

$$\begin{pmatrix}\delta C_{PM}\\ \delta C_{EM}\end{pmatrix} = \begin{pmatrix}f_P\\ f_E\end{pmatrix}\exp(\omega_M t)\sin\left(\frac{m_1\pi x}{d}\right)\sin\left(\frac{m_2\pi y}{d}\right) \times \sin\left(\frac{m_3\pi z}{d}\right) \tag{11}$$

where $\mathbf{f}_P$ and $\mathbf{f}_E$ are the amplitudes and ω_M the eigenfrequencies for the different modes given by m_1, m_2 and m_3 which take non-zero integral values. Substituting in Eq. (10) gives after a few algebraic manipulations

$$\left[\begin{pmatrix}A_{11} - I\omega_M & A_{12}\\ A_{21} & A_{22} - I\omega_M\end{pmatrix} + \begin{pmatrix}DM^2 & 0\\ 0 & 0\end{pmatrix}\right]\begin{pmatrix}f_P\\ f_E\end{pmatrix} = 0 \tag{12}$$

where I is a 2×2 unit matrix and

$$M^2 = (\pi^2/d^2)(m_1^2 + m_2^2 + m_3^2) \tag{13}$$

a term obtained due to the operation by the Laplace operator. As mentioned earlier the interest is in the behaviour of the point defects and, therefore, the above equations can be partitioned using standard techniques to give an equation involving only the point defect amplitudes,

$$[(A_{11} - I\omega_M) - A_{12}(A_{22} - I\omega_M)^{-1}A_{21} + DM^2]\mathbf{f}_P = 0 \tag{14}$$

which will have a non-trivial solution if

$$\det|(A_{11} - I\omega_M) - A_{12}(A_{22} - I\omega_M)^{-1}A_{21} - D^2_M| = 0 \tag{15}$$

The above equation defines the eigenfrequencies for the various modes M^2 as a function of the parameters and sink densities of the homogeneous steady state which are contained in the A matrices. The term $A_{12}\,(A_{22} - I\omega_M)^{-1}A_{21}$ is the additional "interaction", which arises due to the response of the microstructure to the deviation in the point defect concentrations. The physical origin of this term can be understood by drawing an analogy with a molecular impurity in a crystal whose vibrational modes are of interest.[90,91] It is usual in such problems to divide the crystal into two regions: region 1 containing the molecular impurity and the neighbouring atoms forming a pseudo-molecule and the rest of the crystal forming region 2. In this case region 2 (which plays the same role as the extended defect structure) influences the vibrational frequencies of the pseudo-molecule. However, the eigenfrequencies of the system can be obtained exactly by restricting the analysis to region 1 but including an additional interaction which is obtained by following a similar partitioning technique.[90] In the present analysis we are interested in examining if for some microstructural conditions one of the eigenfrequencies of the system becomes soft, setting $\omega_M = 0$ and expanding the determinant in Eq. (15) gives[69]

$$AM^4 + BM^2 + C = 0 \tag{16}$$

where

$$A = D_V D_I \tag{17}$$

$$B = D_V D_I\{3\rho_s - (Z_I + 1)\rho_d\} - Z_I\rho_V(r_s\dot{r}_s/b\dot{r}_V) + \alpha(D_V C_{V0} + D_I C_{I0}) \tag{18}$$

$$\begin{aligned} C = {} & D_V D_I\{(Z_I+1)\rho_s\rho_V + (Z_I+1)\rho_s\rho_d + \rho_l\rho_d \\ & + 2\rho_s^2 + Z_I\rho_d^2\} \\ & + (Z_I - 1)D_V D_I\rho_s\rho_V(D_V C_{V0} + Z_I D_I C_{I0})/b\dot{r}_V \\ & + D_V D_I\rho_s\rho_d(Z_I D_V C_{V0} - D_I C_{I0})/r_s\dot{r}_s \\ & + 2\alpha\rho_s(D_V C_{V0} + D_I C_{I0}) \\ & + \alpha\rho_d(D_V C_{V0} + Z_I D_I C_{I0}) \end{aligned} \tag{19}$$

Equation (16) together with the coefficients defined by Eqs. (17)–(19) is the main equation on the basis of which the kinetic conditions for ordering can be obtained. These conditions will be discussed in the next subsection.

3.1.3 *Discussion of the superlattice properties on the basis of the microstructural instability model*

The kinetic conditions for ordering and a comparison with the experimental observations can be made with the help of Eq. (16). It must be remembered, however, that the equation has been derived for a homogeneous lossy medium and not the real physical system. This equation only gives the onset of ordering or the first bifurcation and not the subsequent time development of the system. Despite these limitations, it is possible to understand many features of the ordering process and these are discussed below.

a) *Onset of ordering*: Experimentally it is observed that the voids are initially randomly distributed and subsequently order. This is an essential feature of the model which views the superlattice formation as a nonequilibrium transition from a disordered to an ordered state. The onset of the ordering commences when Eq. (16) has physical valid solutions with $M^2 \geqslant 0$. In Eq. (16) the coefficients of M^2 are functions of the sink densities ρ_s, ρ_l and ρ_d, and therefore a positive value of M^2 is not assured for any given value of the sink densities. Figure 7 reproduces the phase diagram plot as a function of ρ_s and ρ_V (ρ_d constant) showing the disordered region where no positive solution of M^2 exists and the ordered region where $M^2 \geqslant 0$ solutions are possible. The phase line gives the critical dislocation densities ρ_{sc} and ρ_{Vc} where the first bifurcation or the onset of ordering commences. From the figure it is clear that the system has to evolve through the disordered phase (lower values of ρ_s) before the ordering commences.

b) *Microstructural conditions for ordering*: In the phase diagram in Figure 7, the phase line (ρ_{sc}, ρ_{Vc}) is defined by the $M^2 = 0$ solutions of Eq. (16). This means that the coefficient C must be equal to zero along the phase line. From the expression for C given by Eq. (19) it may be observed that the only term which can become negative is

$$(Z_I - 1)D_V D_I\rho_s\rho_V(D_V C_{V0} + Z_I D_I C_{I0})/b\dot{r} = S \tag{20}$$

Since $\dot{r}_l$ is the rate of vacancy loop shrinkage and hence $\dot{r}_V < 0$. ($Z_I D_V C_{V0} - D_I C_{I0}$ is positive because $Z_I > 1$ and $D_V C_{V0} - D_I C_{I0} > 0$ being proportional to the void growth rate $\dot{r}_s > 0$.) The ordering therefore commences when S becomes equal to or greater than all the other terms added together in Eq. (19). The term S is proportional to the product $\rho_s\rho_V$, and if either of these two sink densities is zero an instability cannot develop in the system. The production of vacancy loops together with voids is, therefore, an important condition for a bifurcation in the microstructural model.

This result is in agreement with the experimental observation that void lattice formation in metals (Group I) has only been observed by neutron or ion irradiation and not by electron irradiation[25] since no vacancy loops are formed in the latter case. It has already been mentioned that interstitial loops which are formed during electron irradiation do not have the required nonlinear coupling with point defects to induce an instability. Another important question which arises is, should vacancy loop ordering be observed together with void ordering during neutron and ion irradiation? If vacancy loop ordering has to occur at all it is with respect to the concentration N_V of the vacancy loops which does not imply that the vacancy loops will be spatially ordered. However, as in the case of voids, the host lattice anisotropy and loop–loop interaction if sufficiently strong could lead to a spatial ordering of loops which would be observed together with the periodic concentration variation. Since a large local concentration of loops is a consequence of a large (local) lifetime of the vacancy loops, one of the possibilities is that vacancy loops may survive only in regions where the lifetimes are large and in this case they will appear to be bunched in groups, and the groups will

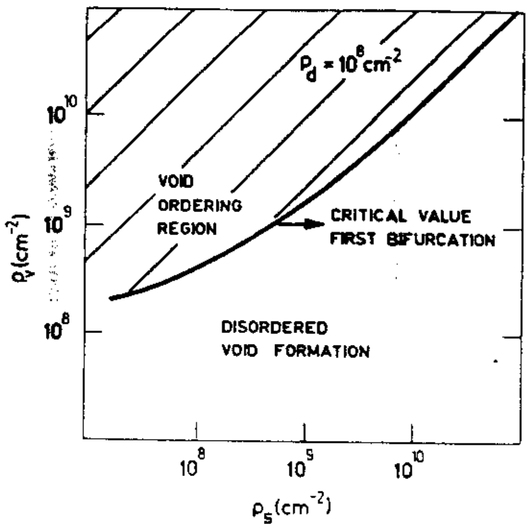

FIGURE 7 Phase diagram showing the ordered and disordered regions as a function of sink densities (from Ref. 57).

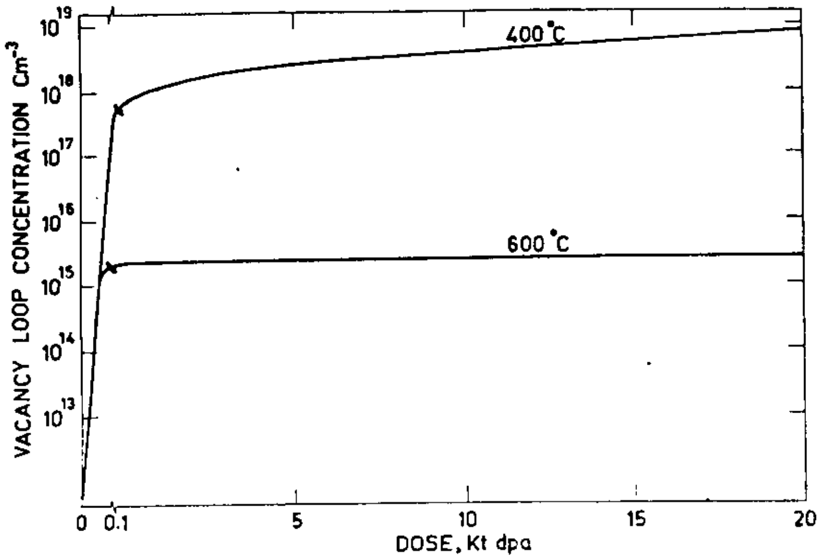

FIGURE 8 Vacancy loop concentration as a function of dose showing saturation at high temperatures and a steady monotonic increase at lower temperatures where bias effects dominate the loop shrinkage mechanism. The calculations are typical of Ni and stainless steel.

not dominate. Temperatures which are just below the peak swelling values will be most favourable for void ordering. These general conclusions are supported by the experimental observations discussed in Section 2.

e) *Estimate of the lattice spacing*: The precise value of the lattice spacing which emerges depends on the evolution of the system beyond the first bifurcation. In this region the linear instability analysis is strictly not valid. However, an estimate can be made from Eq. (16) by examining the functional dependence of M^2 on the sink densities. This is shown in Figure 9, where M^2 as a function of ρ_v rises very sharply across the transition and saturates at a value of 5×10^{11} cm^{-2}. If we assume that the solutions still have the same structure as in Eq. (11) and $m_1 \simeq m_2 \simeq m_3 \simeq m$, $d \sim 10^{-3}$ cm then this value of M^2 can be related to m using Eq. (13) which gives the number of modes m for a wavelength λ_m in a grain of size d. An estimate[69] gives $m \simeq 130$ or an intervoid spacing of the order of 600 Å. The roots of M^2 obtained from Eq. (16) are functions of ρ_s, ρ_v, ρ_d and temperature. The temperature dependence arises due to three factors; (1) the diffusion co efficients, (2) nucleation of voids or void concentration, and (3) the thermal emission of vacancies from the microstructure. (The last process has not been included in the expressions given for A, B and C in Eqs. (17)–(19) but is considered in the numerical calculations.) The dependence of the saturation value of M^2 or equivalently m on ρ_s, ρ_v, ρ_d and T is quite complex. The main results can be summarized as follows. The number of modes m (inversely proportional to the lattice spacing) shows a weak dependence on the network dislocation density ρ_d. It increases with higher values of ρ_s or void concentration and also increases as a function of temperature but only for low void concentrations: at higher concentrations, it tends to become independent of temperature. Though these features are in qualitative agreement with the experimental results, they are, however, open to criticism because of the extension of the model into a regime where it is not applicable. Also numerical calculations show that M^2 change very sharply across the transition, however, it does not completely saturate though there is an abrupt change in slope at the transition.

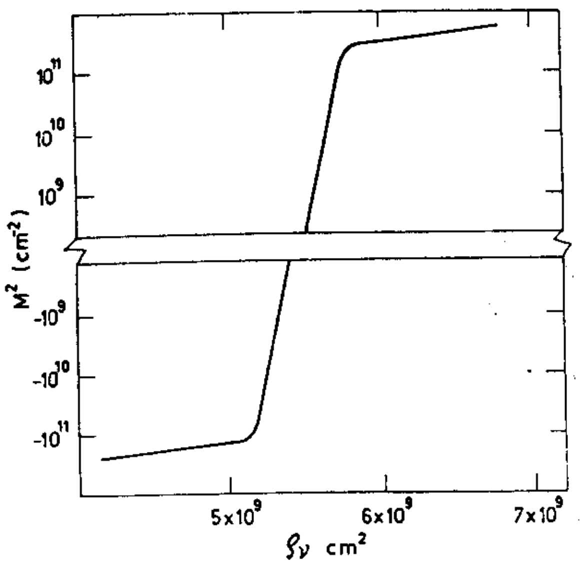

FIGURE 9 The sharp transition at the instability obtained by solving Eq. (16) as a function of the control parameter. The saturation value gives an estimate of the void lattice spacing (from Ref. 69).

f) *Dose and dose-rate dependence*: The dose and dose-rate dependence appear implicity through the microstructural sink densities and the quasi-steady state concentrations of the point defects. In Eq. (19) for C, in the sink dominant regime, the contribution due to the recombination terms involving a can be neglected. The remaining terms (positive terms and the negative term s) involve bilinear product of the sink densities ρ_s, ρ_v and ρ_d. This means that as a function of dose or dose rate the instability depends only on the relative magnitudes and not the absolute value of the sink densities. Therefore, there is no unique critical dose or dose rate for which the ordering occurs but depends on how the various sink densities evolve during irradiation.

g) *Symmetry and stability*: Both these aspects involve an analysis of the evolution of the system after the first bifurcation. It was explained earlier that during this stage the system is driven by fluctuations, the discrete nature of the host lattice and the anisotropy effects it introduces in the diffusion and defect interactions become important. There is at present a limitation in incorporating these features into the mathematical framework of the instability analysis. These effects are, therefore, discussed separately in Section 4.

3.2 *A Recombination Instability: A Possible Mechanism in other Systems—Groups II, III and IV*

It is apparent that the instability mechanism discussed in the previous section cannot explain the observed ordering of voids in stainless steel[53] and in compounds[25] like CaF_2 since these involve electron irradiation which does not produce cascades. It has also been shown[96] that 30 keV He ion irradiation will not result in any significant cascade damage and in this respect the group II, III and IV experiments share a common feature. There are also other similarities in these experiments which are not observed in the case of void ordering in metals These are:

1) The presence and diffusion of gas atom interstitials is involved and is essential for ordering.

2) Ordering is observed at *room* and higher temperatures (though in stainless steel,[53] there was only evidence for spatial regularity after low temperature irradiation ~500°C).

3) Superlattice parameters show no (or weak) temperature dependence.[56]

4) The vacancy mobility at the observed ordering temperatures is low.

5) Superlattice spacing is relatively smaller (60–80 Å for bubbles and ~250 Å for steel and CaF_2 as compared to 200–1500 Å in metals).

6) Electron diffraction studies show that a short range ordering characterized by halo diffraction rings precedes long-range ordering with well-defined diffraction spots.

Though the significance of the above observations is not clearly understood, they show a remarkable similarity with some recent studies in electron irradiated Ni–Cu alloy.[7] In this case, during irradiation an instability causes a long-range spatial composition fluctuation of the alloy elements. In the Cu–Ni alloy a miscibility gap[99] is predicted below 327°C. A phase separation below 327°C is not observed presumably due to the very low thermal diffusion. However, a periodic decomposition is observed between room temperature and 207°C by 3 MeV electron irradiation.[7,100] Initially a short-range ordering is observed and this is reported to be consistent with the model of clustering by Cook.[101] This is followed by a long-range periodic concentration fluctuation which does not show the characteristics of a thermodynamic spinodal decomposition and cannot be explained[7] on the basis of the existing models.[102,103] It has therefore been suggested that an irradiation-induced mechanism may be involved. The main characteristics of this decomposition are as follows.[7] (1) Ordering occurs at *room* and higher temperatures. (2) The wavelength of the fluctuation is independent of temperature and dose. (3) The vacancy mobility is low. (4) The periodicity or wavelength of 45 Å emerges. (5) Short-range clustering precedes long-range periodic fluctuations. These characteristics show a remarkable similarity with those mentioned earlier, particularly in connection with the properties of bubble lattices.[33]

Krishan and Abromeit[97] have recently suggested a mechanism for the instability induced by irradiation in a concentrated AB alloy. The basic physical features of this model are as follows. Since an alloy is never *ideally* homogeneous it can be characterized by a parameter η which describes the presence of a random distribution of A-rich zones in an AB matrix. The irradiation produces A and B interstitials which are mobile and under the dynamic irradiation conditions recombine with the relatively less mobile vacancies. An essential feature of the model is to introduce a difference in the recombination of the A and B interstitials with vacancies in the A-rich zones represented by the parameter η. This is achieved by introducing a small *bias effect* in the recombination kinetics. In the A-rich zones the recombination rate of the A interstitials is assumed to be enhanced by an amount proportional to η, i.e. by $\alpha_A\eta$; while for B interstitial it is surpressed by $\alpha_B\eta$. If k_A and k_B are the recombination rates for the homogenized alloy ($\eta = 0$) then for a finite value of η the recombination rates will be given by $(k_A + \alpha_A\eta)I_AV$ and $(k_B - \alpha_B\eta)I_BV$ where I_A and I_B are the A and B interstitial concentrations and V that of the vacancies. Rate equation similar to Eqs. (2) and (3) can be written for I_A and I_B. Using a simple phenomenological picture, a rate equation can also be developed for the microstructural variable η. The A-rich zone grows by the arrival of I_A interstitials at the zone at a rate proportional to ηI_A and shrinks due to B interstitial at a rate proportional to ηI_B. A stability analysis on the lines discussed in Section 3.1.2 which involves the deviations δI_A, δI_B and $\delta\eta$ shows that a soft mode instability occurs and the growth of the random A-rich zones for a critical value of η gives rise to a long-range periodic concentration fluctuation with a *temperature and dose independent* wavelength.

It is useful to compare the physical processes involved in the above instability with those discussed earlier for the case of void ordering in metals. Though the physical model involves the recombination term, the non-linearity arises due to the bi-linear coupling of the microstructural variable with the point defect concentrations involving the products ηI_A and ηI_B. This is very similar to the non-linearity of the sink terms $\beta_I C_I$ and $\beta_V C_V$ in Eqs. (2) and (3). The variable η plays a role which is similar to the vacancy loops and also obeys a very similar equation. A more detailed analysis shows that the bifurcation occurs as η increases and the rate $\dot{\eta}$ decreases, a situation very similar to the one encountered for vacancy loops. This therefore establishes that despite the different physical processes involved, the factors which lead to the instability are very similar to those encountered in the case of the void lattice. The microstructural instability model is therefore extremely general and can manifest in different physical systems in various ways but the underlying mechanism is similar.[96] The differences in the temperature dependences and the scale of wavelengths observed depend on the microstructural variables involved. Also the temperature dependence of the sink term is different from that involved in the recombination term, which gives rise to the non-linearity in the two respective cases.

The spatial ordering of voids and bubbles has not been examined on the basis of an instability analysis in the case of group II, III and IV experiments. There appears to be in the case of group II and III studies some connection with an instability mechanism discussed for a concentrated AB alloy. In this case the two interstitials involved are the self-interstitials and the gas atom interstitials. However, since the instability model requires a recombination of the vacancies and the interstitials, a strong coupling between the vacancies and gas atom interstitials is required together with the ability for the gas atoms to diffuse. What is the experimental evidence for this? There is now some understanding from theoretical calculations[104] and desorption studies[105,106] regarding the diffusion of He in metals. These results have been recently summarized by Schilling[27] and we give the main conclusions. In fcc metals Ni, Au, Al helium occupies predominantly a substitutional site while for bcc metals Mo and W the evidence is more for interstitial occupancy particularly at higher temperatures. In the case of Ni the He migrate by a dissociative process where He jumps from a substitutional to an interstitial site till it gets retrapped by a vacancy. In Al the binding with a vacancy is very strong and as such a dissociation is not possible which limits the diffusion by a vacancy-assisted process. The behaviour of Ni is expected to be very representative of stainless steel where similar processes can be expected.[107] Also in Cu vacancies have a high probability of trapping He atoms and the behaviour is expected to be very similar to Ni.[96] In Mo and W though the interstitial migration is expected at high temperatures there exists a strong binding of the He atoms with the vacancies.[27] From this we see that in fcc metals Ni, Cu and stainless steel and bcc Mo, in all of which helium bubble lattices are observed, a strong binding between the vacancies and gas atoms is reported. An instability of the type discussed in this section involving the recombination mechanism could be responsible for inducing the ordering. Such an instability would also be consistent with the observation that the average bubble size and lattice spacing increases due to electron irradiation in a superlattice previously formed by light gaseous ion irradiation.[34]

In the case of compounds like CaF_2 it is difficult to say whether a similar instability mechanism operates. Due to the process of damage involved,[25] only one interstitial (namely fluorine atoms) is produced as a result of irradiation. However, the formation of calcium crystallites requires the aggregation of calcium atoms. There is, therefore, again a possibility that an irradiation-produced vacancy recombines with a neighbouring calcium atom or a fluorine interstitial making the process very similar to the case of bubble-lattices.

3.3 *Instability Due to Diffusion Terms and Point Defect Interactions*

Benoist and Martin[108] were the first to point out that the formation of the void lattice may be viewed as a self-organization process involving a dissipative system moved far from equilibrium. They have developed a kinetic model for the *stability* of the void lattice and this will be discussed in Section 4. Though no detailed application to the case of void lattice formation has been reported, they have given a possible criteria for the ordering to occur. This is based on the dissipation of the formation energy of the Frenkel pairs in the form of heat and surface energy of voids. They have argued that this dissipation is maximum when the voids are arranged in an ordered lattice.[108]

Martin[80,87,109] and coworkers[106,111] have also discussed other physical models which can lead to spatial instabilities in solids during irradiation. Their treatment is general and covers ordered defect arrays and radiation induced precipitation, though a specific application to the case of void lattice formation has not been made. Nevertheless, it is instructive to examine the cause of the instability in Martin's model (called henceforth M-instability) and its relation with the microstructural instability in Krishan's model (K-instability) which was discussed in the earlier sections. It was mentioned earlier that the two coupled rate Eqs. (2) and (3) are stable if the sink densities β_I and β_V are regarded as quasi-stationary. The M-instability arises by modifying the diffusion terms $D_V\nabla^2 C_V$ and $D_I\nabla^2 C_I$. This is done in two ways. Firstly it is argued that the contribution to the diffusion processes involves, in addition to the normal Ficks term, an additional drift force Fp on vacancies and interstitials such that [86,87]

$$\left.\frac{\partial Cp}{\partial t}\right|_{\text{diffusion}} = Dp\left[\nabla^2 Cp - \frac{\nabla\cdot Fp\,Cp}{\Omega k_B T}\right] \tag{21}$$

The suffix p (or q) stands for the diffusing species and in particular V and I. The origin of this drift force arises from the basic interactions between point defects of the type V–I, V–V and I–I for which a phenomenological potential of the type $\exp(-r^2)/r^2$ is used.[87] In the second approach it is assumed that diffusion of the various defect species is interdependent so that [109,110]

$$\left.\frac{\partial Cp}{\partial t}\right|_{\text{diffusion}} = -\nabla\cdot J_p \tag{22}$$

and

$$J_p = \sum_q f_{p,q}\nabla C_q \tag{23}$$

J_p is the flux for a specific point defect type and from Eq. (23) this flux is coupled linearly through the functions $f_{p,q}$ to the gradients in the concentrations. The $f_{p,q}$ therefore are related to the phenomenological Onsager's coefficients and involve the diagonal and off-diagonal terms in the diffusion matrix. In both these approaches the net result is to introduce off-diagonal elements into the diffusion matrix D in the condition for instability derived in Eq. (15). The M-instability is induced in Eq. (15) if the off-diagonal elements in the D matrix have appropriate signs while in the K-instability the matrix is diagonal but the off-diagonal coupling arises due to the coupling with the microstructure in the term $A_{12}(\omega A - I\,\omega_M)^{-1}A_{21}$. In the M-instability the non-linearity arises due to the recombination term $\alpha C_V C_I$ while in the case of the K-instability the non-linearity is ascribed to the sink terms $\beta_I C_V$ and $\beta_I C_I$. Though a detailed application of the M-instability model has not been made for the case of the void lattice to allow for a more detailed comparison, it is apparent that there is an important difference in the physical processes which are involved in the two models. In one respect, however, there may be an important connection, the K-instability and the M-instability arise due to the difference in the behaviour between the vacancy and the interstitial. In the K-instability this effect is included in the bias term Z_I in the absence of which ($Z_I = 1$) the instability does not occur. In a sense, in the case of the M-instability, a similar difference between the point defects gives rise to the off-diagonal terms in the diffusion matrix. It is for this reason that both these models can also be used to describe spatial instabilities in alloys[97,110] and a connection may exist between these different approaches.[112]

Imada[85] has also proposed a void lattice model on similar lines. In this model the ordering is produced due to a spinodal type decomposition of the vacancy concentration. Except for vacancies no other point defects or extended defects are involved. The instability arises due to the vacancy–vacancy interaction, which is assumed to be sufficiently strong so that an uphill diffusion of vacancies is possible. The model shows that the wavelength is larger for larger diffusion constants. However, the model does not explain many of the other characteristics of void ordering.

4 ANISOTROPY EFFECTS AND SUPERLATTICE ENERGY CONSIDERATIONS

4.1 *Anisotropy and Void–Void Interactions*

The related symmetries of the superlattice and the host lattice suggest that the discrete nature of the host lattice must manifest itself during some stage of the ordering process. The rate equations used in the instability analysis contain no information about the host lattice structure and as such can only explain the kinetic conditions for the onset of ordering. Once the instability develops the inherent fluctuations will no longer be damped but will grow in time driving the system from the homogeneous (disordered) state to one with a *lower* symmetry, namely the ordered lattice. The instability only dictates the scale length that determines the wavelength which will dominate in the system but not the precise symmetry. During this stage of evolution the voids will (1) shrink and grow at selective spatial regions, and (2) the spatial fluctuations in the point defect concentrations will lead to a Brownian type motion which will be influenced by the host matrix anisotropy and this will eventually lead to a specific superlattice symmetry. Two mechanisms have been proposed for explaining this symmetry. These are by Malen and Bullough[85] based on the void–void interactions and by Foreman[83] who considers the anisotropic interstitial diffusion arising from replacement collisions. Both these mechanisms are discussed below.

Willis and Bullough[113] have shown that in an elastically isotropic solid the interaction between two voids (or gas bubbles) is attractive at all distances. Since a repulsive contribution is required to stabilize the void lattice, Malen and Bullough proposed that the host-lattice elastic anisotropy

$$\delta = C_{11} - C_{12} - 2C_{44}$$

(where C_{11}, C_{12} and C_{44} are the elastic constants) must be responsible for the repulsive interaction. By using a real space Green's function method they have shown that the interaction between two voids separated by a distance R is given by

$$E(R) = -\frac{8p^{*2}(1-\beta)^2\delta}{3r_v^2 C_{44}^2}\left\{\left(\frac{r_v}{R}\right)^3 - \frac{28C_{44}}{9\delta(1-\beta)}\left(\frac{r_v}{R}\right)^5\right\}\left\{3 - \frac{5(x^4+y^4+z^4)}{R^4}\right\} \tag{24}$$

where $\beta = (C_{12} - C_{44})/(C_{12} + 2C_{44})$, r_v is the void radius and p^* can be related to the force distribution which represents the faceted character of the voids. The above expression can be used to calculate the energy per void by summing over various shells for any given superlattice arrangement of voids. Malen and Bullough assumed a bcc superlattice with spacing D and summed till 25 shells. The energy depends on the ratio D/r_v and for Mo it was a minimum for $D/r_v = 3$ for spherinial voids and $D/r_v = 8$ for faceted voids. Stoneham[114] with the same physical model has used a Fourier representation which enables an exact evolution of the superlattice energy. The void is represented by a system of forces $F_\alpha^*(r)$, $\alpha = x, y, z$, suitably taken to represent the faceting of the voids. The void lattice with an assumed symmetry is represented by a force field which in the Fourier transformed space q is given by

$$F_\alpha(q) = \sum_j{}' \exp(i\,q\cdot L_j)\sum_r \exp(i\,q\cdot r)\,F_\alpha^*(r) \tag{25}$$

where $\mathbf{L}_j$ are the co-ordinates of the voids in the lattice and the prime indicates that $j \neq 0$. Using the anistropic perfect lattice Green's function $G_{\alpha\beta}(q)$ the elastic energy is given by

$$E = -\frac{1}{2N_v}\sum_q F_\alpha(q)\,G_{\alpha\beta}(q)\,F_\beta(-q) \tag{26}$$

where N_v is the number of voids per unit volume and the sum over q is finite being restricted to the first Brillouin zone of the host lattice. Stoneham has done calculations for various force arrays to simulate void faceting and finds that in Mo the ratio D/r_v varies from 2.2 to 4.5 in comparison to 10 which is experimentally observed. Calculations were also done for different void lattice symmetries. the lowest energy was for bcc followed by fcc and hcp. In the case of a simple cubic lattice no minimum was obtained. The low value of D/r_v was accounted for subsequently by Tewary and Bullough[115] by using a defect Green's function instead of the perfect lattice Green's function used in earlier calculations. The former takes into account the changes in the host lattice force constants due to the presence of defects and also corrects for the phonon dispersion. These modifications in the calculations give a D/r_v of 10 in agreement with experiments and also a binding energy of 0.5 eV per void. An extension of these results to the case of Ta and V has been done by Tewary.[116] The ratio D/r_v is in agreement with experiments for Ta for which a high thermal stability is predicted but no observation for void ordering in V have been reported so far.

The anisotropy-induced void lattice model has many appealing features. It emphasizes the connection between the host lattice and the void lattice, predicts a temperature and dose independent ratio for D/r_v and explains the thermal stability of the void lattice. However, it is in the overall application of the theory to a wider class of materials and to the kinetics of the ordering process that limitations become apparent. It is difficult to understand why if ordering depends entirely on the material properties alone (like anisotropy) superlattices are generally not found by electron irradiation. Also an interaction model for voids assumes that voids can move to minimum energy site positions. There have been no experimental observations which suggests that voids can move. In CaF_2 though such movement is observed[10,118] its Brownian-motion-like nature suggests that this is related to the spatial instability in the system rather than as a consequence of void interactions. Foreman[63] has also argued that it should be possible to improve the alignment by thermal annealing at high temperatures in cases where the voids are displaced slightly from the perfect lattice positions. Such alignment is not observed experimentally though Evans *et al.*[64] have reported partial alignment of voids in Mo by rapid quenching from high temperatures. Calculations however show that void movement is possible under temperature and stress gradients.[119] Stoneham[15] has also suggested that a surface diffusion controlled mechanism may operate though there is no experimental evidence for this. One of the important predictions of the model is that ordering should occur in materials with a large anisotropy. There appear to be exceptions to this. Void ordering is observed in *W* which is isotropic and this is mentioned as an evidence against the model.[38] The temperature dependence of the anisotropy parameter δ is also not reflected by the temperature dependence of the ratio D/r_s to which it is proportional.[38] Also a void lattice is formed in Ta which has a negative anisotropy though this is not a limitation because the contribution due to void faceting can account for the change in sign as has been done in the calculation by Tewary.[116] In V no void lattice has been observed, though a highly stable lattice is predicted.[116] The faceting of voids and the anisotropy of the surface tension probably plays a more important role than the crystal elastic anisotropy. (Such effects have for example been found to be very important in the case of ordered lattices consisting of stacking fault tetrahedra.[117]) In CaF_2 and SrF_2 the void lattice has a simple cubic symmetry which is only related to the fluorine sublattice. A simple cubic lattice is expected to be unstable in this model and, besides, it is difficult to explain why it should be related only to the fluorite sublattice. Also in this model the symmetry and its orientation with reference to the host matrix is an artifact of the model rather than a consequence of the theory.

Another interesting model which invokes the crystallographic anisotropy of the host lattice is due to Forman.[63] The model is based on the propagation of interstitials as collision replacement sequences or dynamic or static crowdions along favoured crystallographic directions of the host matrix. This amounts to an anisotropic diffusion of the interstitial atoms. When the voids are small this anisotropy is not important since each void acts independently. As they grow to a size comparable to the intervoid spacing ($D/r_s \sim 5$–15) they start shadowing each other from the interstitial fluxes. The voids which are in the shadow region grow while the others shrink, due to the absorption of interstitials. As a consequence of this shadowing effect, voids tend to align with the symmetry and orientation dictated by the host lattice. The model is therefore capable of explaining qualitatively the observed connection between the void and the host lattice, order of magnitude of the D/r_s ratio, difference between bcc and fcc metals, and the dependence on the nature of the irradiation. Perhaps the most direct support for the model comes from the observation of ordering in compounds like CaF_2. In this case, as has been argued by Chadderton *et al.*,[24,25] the model is particularly attractive because the simple cubic superlattice seems to be mainly related to the fluorine sublattice which is formed as a result of ⟨100⟩ focuson collisions. The 100 keV electron irradiation has insufficient energy to directly displace either the calcium or fluorine atoms.

There are two main difficulties in the Foreman model. Firstly, the focussed replacement sequences must propagate to distances which are at least twice the spacing between voids. Superlattices of voids and bubbles have been observed with spacings ranging from 60 Å to over 1500 Å the latter being in Nb at high temperatures.[44] If the Foreman mechanism was the only mechanism in all these cases, then it would require focussed replacement sequences to be over 2000 Å long: these should be stable even at reasonably high temperatures and also in alloys. There is no experimental or theoretical[120] evidence to support this and therefore this mechanism would be more effective only in superlattices with a small lattice spacing. Secondly, the mechanism can operate effectively only if partial ordering has already developed. Starting from a completely random distribution it is difficult to conceive how a long-ranged ordering can develop throughout the grain. Also the stability of the replacement sequences would be effected by the presence of voids.

If the Malen and Bullough and the Foreman mechanisms are viewed in the broader perspective

of the microstructural instability model the above-mentioned limitations of both the models can be resolved. Both these mechanisms form a part of the more general process of ordering and must be viewed as mechanisms which contribute to the stability and alignment of the void lattice once the kinetic conditions favour the process of ordering. In the absence of an instability the void movement is hindered, but once the process of ordering commences the void–void interactions contribute to the stability and as *partial ordering* is developed the anisotropic interstitial diffusion will contribute to an improved alignment. The experimental observations of Chadderton *et al.*[25] in compounds like CaF_2 are particularly significant and appear to support this viewpoint. The manifestation of the Foreman mechanism in CaF_2 has been discussed by Chadderton *et al.* and also in this article. There is one observation, however, which indirectly shows the significance of elastic forces. Amongst the compounds CaF_2, SrF_2, BaF_2 and alkali halides an ordered lattice has only been observed in CaF_2 and in SrF_2 though voids form in all these systems. It has been shown that only in the case of CaF_2 can the calcium crystallites be coherently accommodated in the CaF_2 matrix because of the comparable lattice parameters. In SrF_2 the lattice parameters are slightly different and form an imperfect lattice, the voids showing a strain contrast. In the other cases no ordering is observed because the metal crystallites precipitate incoherently. Though this does not establish any positive evidence for ordering due to elastic interactions, it nevertheless shows that elastic strain interactions are important and a Foreman-type mechanism is not the *only* determining factor in the ordering process. One of the effects due to the strain fields would be to make voids immobile under the elastic interaction influences in the presence of the instability in the system.

4.2 *Other Models for Void Ordering*

Several other mechanisms have been proposed for void ordering. These, however, seem to be limited in their scope and application. These mechanisms have been reviewed by Stoneham[8,15] and therefore no detailed account will be given here. Nolfi[121,122] has shown that the interactions arising from the segregation of misfitting solutes or impurities on void surfaces can give rise to the repulsive and attractive features in the potential so that an ordered lattice has a minimum energy. This model is based on the observations of Loomis *et al.*[44] who found a threshold oxygen concentration as a prerequisite for ordering in Nb. Though some of the observations like the D/r_s ratio can be explained, the model predicts a strong binding only with increasing temperature contrary to observations. A strong strain field associated with the voids due to a solute shell around the void would also effect void mobility and hence inhibit void ordering, as is clearly shown by the difference in the behaviour of CaF_2, SrF_2 and BaF_2.[24,25] In this respect the suggestion of Loomis *et al.*[44] that a strong binding between the vacancy and solute impurity may be important, is pertinent in view of the discussion on the recombination induced instability in Section 3.2.

Another mechanism has been proposed by Brown.[123] The model assumes a steady state attained by the system by minimizing the total energy stored as point defects and as surface energy of voids which provide the main sink for the point defects. It has been pointed out by Seidman and Balluffi[124] that such a minimization criteria cannot be applied to a highly non-equilibrium system. Subsequently Norris and Brown[125] have improved the model by taking into account point defect recombination and loss to other sinks. They conclude that though the new minimum energy criteria is relevant it cannot explain void ordering or saturation in swelling. Also Winter[126] has suggested that a bcc lattice is most favoured because the bcc structure gives the most economical path length for vacancies to travel. However, vacancy diffusion does not seem to be a limiting parameter in void ordering and other symmetries besides bcc have been observed. Lucas[127,128] has given a model where he envisages a void–void interaction based on plasmon fluctuations, which contribute to surface energy of metals. This model also has inconsistencies which have been pointed out by Stoneham.[8]

4.3 *Superlattice Stability*

There are two aspects to the stability of the void lattice; stability during thermal annealing and stability during irradiation.

Tewary and Bullough[115] have examined the thermal stability of the void lattice in Mo where it is found that the vacancy evaporation from voids commences at 1500°C in a lattice as against 1100°C for an isolated void. They have related the stability to the void–void interaction which places each void in a lattice in a minimum energy well approximately 0.5 eV deep. From the curvature of the energy minimum they derive the lattice compressibility and find that the energy required for the void lattice to shrink or expand by releasing one vacancy per void accounts for a rise of approximately 450°C in its thermal stability. The same argument can be extended to account for the irradiation stability of the void lattice. The extension[116] of these results to Ta and V, however, gives a minimum energy of 1.35 eV and 10 eV respectively which would give an anomolously high stability particularly for V (where a void lattice is not observed).

A kinetic criteria for the stability has been given independently by Benoist and Martin[108] and by Ryazanov and Maximov.[129-131] The mechanism is based on the anisotropic point defect fluxes which arise when a void is displaced from its perfect lattice site. The fluxes are directed so that the void preferentially grows in the direction of the perfect lattice site, the alignment is increased and favours ordering. The point defect diffusion fields therefore introduce a "repulsive force". This force depends on the superlattice symmetry and was shown to be favourable for bcc and fcc arrangements.[108] However, it seems that a criterion on these lines cannot explain the *alignment* of the superlattice symmetry with that of the host lattice, and therefore either a mechanism like the one discussed by Foreman has to be invoked or the faceting of voids plays the determining role. Also the diffusion interaction mechanism has the same limitation as in the anisotropic interstitial diffusion model of Foreman; it can explain the improved alignment but canot lead to an ordered structure starting from a disordered array.

The treatment by Ryazanov and Maxinov[129] includes the presence of other sinks and is based on the observation that the void size distribution is highly peaked once the voids order into a lattice. The mechanism, however, is the same as in the case of Benoist and Martin's model, namely, diffusion interaction. If the void size distribution is broad, then the voids smaller than a critical size would evaporate faster and the vacancy flux produced would enable other voids to grow making such a distribution thermally less stable. They, therefore, consider the case when the void radius distribution has a small spread δr_s about an average value r_s and determine the effect of this distribution on the growth of a single void. The void positions are averaged to take into account the anisotropic diffusion fluxes. Their results are summarized in terms of two parameters; the time dependence of $r_s(t)$ and the time dependence of the void size dispersion $\sigma(t)=\delta r_{s,t}^2$. This time dependence is a function of the sink structure in the system. For the thermal stability of the void lattice they find that in the low dislocation density regime, $r_s(t)$ decreases faster than $\sigma(t)$ which stabilizes the lattice while at higher sink densities $\sigma(t)$ and $r_s(t)$ evolve simultaneously as the voids evaporate. The time constants in the two cases are substantially different. A similar argument is extended to the case of the void stability under irradiation. The situation in this case is more complex and depends more critically on the nature of the sink structure. A general criteria for lattice stability in the case when only network dislocations are present and for $K_V \simeq K_I \simeq K$ is [129]

$$\frac{KD^3\ (Z_I-1)}{4\pi a_V} \geqslant 1 \tag{27}$$

where $a_V = D_V C_V^{th} R_t$, C_V^{th} is the thermal vacancy concentration, D the lattice spacing, and R_t is the trapping radius. From a detailed analysis of the point defect diffusion fields they show that for low dislocation densities and in the absence of other traps for the three conditions given by $KD^3(Z_I-1) \lesssim a_V$, no void lattice stability exists since $\sigma(t)$ grows faster than $r_s(t)$. On the other hand for high dislocation density and for the condition $K(Z_I-1)r_s \gtrsim a_I\rho_d$ a stable lattice can emerge but not if $K(Z_I-1)r_s \simeq a_I\rho_d$. The other condition under which a stable lattice can form is in the presence of impurity traps. The presence of vacancy type sinks which have a sufficient binding with vacancies helps in stabilizing the void lattice, while in the case of interstitial atoms it depends on the probability of trapping interstitials.

The results presented in this paper[129] show some similarity with the microstructural instability model.[68] Equation (27), for instance, shows the dependence on the bias (Z_I-1). Also the role of the impurity binding with vacancies becomes apparent. This connection, however, is not very surprising since the basis of the two approaches is the same. In both these models, physically we are looking at the changes in the point defect fluxes brought about due to variations in the microstructural variables. However, two different aspects of the problem are being viewed. In the diffusion interaction model the kinetics of the evolution of the void size distribution $\sigma(t)$ and $r_s(t)$ is examined under the assumption that the system is not influenced by a bifurcation. This assumption may be a valid one since only the local conditions of growth

are important in this analysis. In this respect the diffusion interaction model and the microstructural instability model complement each other. However, in the diffusion model the recombination between vacancies and interstitials has been ignored. Also, the presence of vacancy loops during the dynamic irradiation conditions would alter the diffusion fluxes of vacancies. It is not clear how these two contributions will influence $r_s(t)$ and $\sigma(t)$. The diffusion interaction seems to be very important in explaining why the void lattice develops with a sharp distribution in void sizes which is characteristic of void lattice formation. However, it is not as apparent that a kinetic model such as this should account for the stability. Since the arguments are based on the relative time constants and not energy considerations, it would imply for example that a void lattice should eventually evaporate in Mo between 1100°C and 1500°C if retained for a sufficiently long time at this temperature.

There is one aspect of the microstructural instability model[68] which may provide a clue to the irradiation stability of the void lattice. The 4×4 matrix in Eq. (12) has four solutions for the frequencies ω_M for a given M^2 value obtained from the determinant in Eq. (15). Two of these frequencies are negative and two positive. The positive frequencies arise in the model because both the void radius and the vacancy loop concentration increase with time. A positive value of the frequency must not be interpreted as an instability in the system but arises due to the growth of the microstructure prior to the instability since it has not acquired a steady state condition. At the critical microstructural densities one of these frequencies becomes zero indicating a soft mode. If the calculation is done with a slightly higher value of the microstructural densities[96] for a fixed value of the wavelength λ_M or M^2 this frequency becomes negative. This would, however, imply a higher overall stability of the system. The use of the linear equations beyond the critical sink densities is not strictly justified.

5 SUMMARY AND OUTSTANDING PROBLEMS

In the first part of this article the experimental results on void and bubble ordering in metals and compounds have been reviewed. In the latter part an attempt is made to provide a consistent theoretical framework to explain the experimental observations. The approach followed is perhaps biased in favour of viewing the ordering as a non-equilibrium phase transition. The justification for this viewpoint is that the instability which causes the transition occurs in the BEK-equations which form the basis for the theory of random void growth and no special mechanism is postulated. The conditions for the instability are consistent with the observed kinetic features for ordering. The approach therefore unifies the treatment of void ordering and void growth and links it to a common set of equations. In the case of bubble lattices, where gas atoms are directly involved in the ordering process, it is shown that a similar instability can arise due to the recombination of the self and gas atom interstitials with vacancies. A detailed study of the ordering kinetics has not been made so far in this case, but some of the differences with void ordering in metals can be qualitatively explained. The instability approach is consistent with other models which invoke void–void interactions or crystalline anisotropy. On the other hand, the instability gives the kinetic conditions for which some of these mechanisms will operate and resolves the difficulties in applying these models to a large class of materials.

Despite these advantages there still remain conceptual and mathematical gaps in our understanding which have to be bridged. The description of the evolution of the system after the onset of the instability has been qualitative and very unsatisfactory. The difficulties here are more mathematical than conceptual. A proper treatment of the secondary bifurcations which includes the effects due to crystalline anisotropy is required. This would also bring out the deeper connection between the different factors: elastic anisotropy, void–void interactions, anisotropy in the surface tension of voids, and interstitial diffusion due to replacement sequences, all of which influence the ordering kinetics. In the instability approach it is no longer required that any one of the above factors should be entirely responsible for explaining all aspects of ordering. These factors manifest to different extents depending on the material and environmental conditions. This will perhaps lead to an understanding of the differences between fcc and bcc metals and between low and high temperature behaviour where the degree of alignment is effected. There is also no detailed treatment of the spatial fluctuations and the influence of small quantities of impurity gases which can act as traps for point defects.

An understanding of the ordering of void and bubbles must also lead to an overall picture regarding ordering of different types of defects under various physical conditions. In this article we have encountered lattices of vacancies, interstitials, stacking fault tetrahedra, vacancy loops, voids and bubbles. Is an instability always involved? In some cases the ordering is observed after quenching including in the case of voids where partial ordering has been reported at least in one case. The answer seems to be no. It depends both on the conditions under which the ordering has occurred and the defects involved. Defect interactions are undoubtedly important but unless the defects are mobile under the environmental conditions in which they are formed no ordering can be expected. The approach followed in this article provides a qualitative picture but in some cases detailed calculations are still required.

There is still no clear answer to the two important properties of the void lattice, namely its symmetry and stability. The question of symmetry cannot be answered from a purely instability approach. Void-void interaction and energy considerations can perhaps say that a bcc or fcc structure is favourable in a specific system but cannot explain the alignment. Here it seems that the anisotropy of the surface tension or a proper treatment of void faceting may be required. However, the anisotropic interstitial diffusion due to replacement sequences is equally attractive, particularly in view of the ordering observed in compounds like CaF_2. There have also been many approaches to the problem of stability, but the most plausible appears to be the void-void interactions particularly for thermal stability. The irradiation stability may of course emerge from kinetic considerations and must also lead to an explanation for the saturation effects.

There is also strong evidence that the presence of impurity gases (particularly oxygen, nitrogen and in some cases carbon) aids the ordering process. In the approach followed in this article the presence of such gases enhances the fluctuations since these gases can act as traps for vacancies, producing local chemical fluctuations which eventually lead to a bifurcation of the system. Other mechanisms like the solute segregation interaction have also been proposed. The role of the impurity gases in the ordering processes needs more detailed experimental investigation. Differences are also expected to arise between gases like helium and oxgyen since their complexes with vacancies differ in stability and mobility.

In conclusion, the ordering of voids and bubbles into lattices under irradiation involves a combination of kinetic and energetic considerations. The manifestation of these may depend on the irradiation conditions and material properties, and may involve different physical processes, but the phenomenon has a common underlying similarity. It is only in this broader perspective that it seems possible to unify all the observed facts and to evolve a consistent picture.

ACKNOWLEDGEMENTS

I am extremely grateful to N. S. Thampi for valuable help and for reading the draft manuscript. I would also like to thank North-Holland Publishing Company, Macmillan Journals Ltd. and Taylor and Francis Ltd. for permission to reproduce the figures.

REFERENCES

1. Charles and N. Knight, *Scientific American* **228**, 100 (1973).
2. J. S. Langer, *Rev. Mod. Phys.* **52**, 1 (1980).
3. S. Amelinckx, American Institute of Physics, *Conference Proceedings* **53**, 102 (1979).
4. D. P. Seraphim, N. R. Stemple, and D. T. Novick, *J. Appl. Phys.* **33**, 136 (1962).
5. R. E. Villagrana and G. Thomas, *Phys. Stat. Solidi* **9**, 499 (1965).
6. D. I. Potter, Ph.D. Thesis, University of Illinois.
7. W. Wagner, R. Poerschke, and H. Wollenberger, *J. Phys. F* **12**, 405 (1982).
8. A. M. Stoneham, in *Consultant Symposium, The Physics of Irradiation Produced Voids*, R. S. Nelson (Ed.), AERE-R 7934, p. 319 (1975).
9. P. B. Johnson and D. J. Mazey, *Nature* **276**, 595 (1978).
10. L. T. Chadderton, E. Johnson, and T. Wohlenberg, *Physica Scripta* **13**, 127 (1976).
11. J. D. Weeks and G. H. Gilmer, Dynamics of crystal growth, in *Adv. Chem. Phys.* **40** (1981).
12. J. Van Landuyt and S. Amelinckx, *J. Sol. State Chem.* **6**, 222 (1973).
13. A. M. Stoneham and P. J. Durham, *J. Phys. Chem. Sol.* **34**, 2127 (1973).
14. V. K. Tewary, *J. Phys. F* **3**, 1275 (1973).
15. A. M. Stoneham, in *Proc. Int. Conf. on Fundamental Aspects of Radiation Damage in Metals Vol. 2*, M. T. Robinson and R. W. Young, Jr. (Eds.), CONF-751006, p. 1222 (1975).
16. G. Nicolis and I. Prigogine, *Self-Organization in Nonequilibrium Systems* (John Wiley and Sons, New York, 1977).
17. H. Haken, *Synergetics* (Springer-Verlag, New York, 1975).
18. A. D. Brailsford and R. Bullough, *J. Nucl. Mater.* **44**, 121 (1972).

19. A. D. Brailsford and R. Bullough, *Phil. Mag.* **27**, 29 (1973).
20. R. Bullough, B. Eyre, and K. Krishan, *Proc. R. Soc.* **A346**, 81 (1975).
21. N. M. Ghoniem and G. L. Kuncinski, *Rad. Effects* **41**, 81 (1979).
22. A. D. Brailsford and R. Bullough, Harwell Report AERE-TP 854 (1980).
23. J. Gittus, *Irradiation Effects in Crystalline Solids* (Applied Science Publishers Ltd., London, 1978).
24. L. T. Chadderton, E. Johnson, and T. Wohlenberg, *Rad. Effects* **28**, 111 (1976).
25. L. T. Chadderton, E. Johnson, and T. Wohlenberg, *Comments Sol. State Phys.* **7**, 105 (1976).
26. M. W. Thompson, *Defects and Radiation Damage in Metals* (University Press, Cambridge, 1969).
27. W. Schilling, in *Proc. Yamada Conference V on Point Defects and Defect Interactions in Metals*, Kyoto, Japan (1981), in press.
28. H. Trinkaus and H. Ullmair, *Phil. Mag.* **A39**, 563 (1979).
29. A. Risbet and V. Levy, *J. Nucl. Mater.* **50**, 116 (1974).
30. P. B. Johnson and D. J. Mazey, *Rad. Effects* **53**, 195 (1980).
31. R. S. Nelson, *J. Nucl. Mater.* **88**, 322 (1980).
32. J. H. Evans, *J. Nucl. Mater.* **76** and **77**, 228 (1978).
33. P. B. Johnson and D. J. Mazey, *J. Nucl. Mater.* **95** and **94**, 721 (1980).
34. P. B. Johnson and D. J. Mazey, *Nature* **281**, 359 (1979).
35. J. H. Evans, *Nature* **229**, 403 (1971).
36. J. H. Evans, *Rad. Effects* **10**, 55 (1971).
37. G. L. Kulcinski and J. L. Brimhall, *Ordered Defect Structures in Irradiated Metals*, ASTM-STP 529, p. 258 (1973).
38. F. W. Wiffin, in *Radiation Induced Voids in Metals*, J. W. Corbett and L. C. Ianniello (Eds.), Albany, USAEC-CONF-71061, p. 386 (1972).
39. B. L. Eyre and J. H. Evans, in *Voids Formed by Irradiation of Reactor Materials*, BNES Conf., S. F. Pugh, M. H. Loretto and D. I. R. Norris (Eds.), p. 323 (1971).
40. J. H. Evans, R. Bullough, and A. M. Stoneham, in *Radiation Induced Voids in Metals*, J. W. Corbett and L. C. Ianiello (Eds.), USAEC-CONF-71061, p. 522 (1972).
41. V. K. Sikka and J. Moteff, in *Proc. Int. Symposium on Defects Interactions in Solids*, K. I. Vasu, K. S. Raman, D. H. Sastry, Y. V. R. K. Prasad (Eds.), Bangalore, p. 86 (1972).
42. J. Moteff, V. K. Sikka, and H. Jang, in *Consultant Symposium, The Physics of Irradiation Produced Voids*, R. S. Nelson (Ed.), AERE-R 7934, p. 181 (1975).
43. L. J. Chen and A. J. Ardell, *J. Nucl. Mater.* **75**, 177 (1978).
44. B. A. Loomis, S. B. Gerber, and A. Taylor, *J. Nucl. Mater.* **68**, 19 (1977).
45. H. Jang and J. Moteff, in *Proc. Int. Conf. on Radiation Effects and Tritium Technology for Fusion Reactors*, J. S. Watson and F. W. Wiffen (Eds.), CONF-750989, pp. 1-106 (1976).
46. J. L. Brimhall and G. L. Kulcinski, *Rad. Effects* **20**, 25 (1973).
47. B. A. Loomis, A. Taylor, and S. B. Gerber, in *Proc. Int. Conf. on Fundamental Aspects of Radiation Damage in Metals, Vol. 2*, M. T. Robinson and R. W. Young, Jr. (Eds.), CONF-751006, p. 1245 (1975).
48. V. K. Sikka and J. Moteff, *J. App. Phys.* **43**, 4942 (1972).
49. G. L. Kulcinski, J. L. Brimhall, and H. E. Kissinger, in *Radiation Induced Voids in Metals*, J. W. Corbett and L. C. Ianiello (Eds.), Albany, USAEC-CONF-71061, p. 449 (1972).
50. G. L. Kulcinski, J. L. Brimhall, and H. E. Kissinger, *J. Nucl. Mater.* **40**, 166 (1971).
51. D. J. Mazey, S. Francis, and A. Hudson, *J. Nucl. Mater.* **47**, 137 (1973).
52. V. K. Sikka and J. Moteff, *Cryst. Lat. Def.* **3**, 113 (1972).
53. S. B. Fischer and K. R. Williams, *Rad. Effects* **32**, 123 (1977).
54. P. B. Johnson and D. J. Mazey, *J. Nucl. Mater.* **64**, 145 (1977).
55. S. L. Sass and B. L. Eyre, *Phil. Mag.* **27**, 1447 (1973).
56. D. J. Mazey, B. L. Eyre, J. H. Evans, S. K. Erents, and G. M. McCraken, *J. Nucl. Mater.* **64**, 145 (1977).
57. K. Krishan, *Nature* **287**, 420 (1980).
58. J. H. Evans, R. Bullough, and A. M. Stoneham, Harwell Report, AERE-6647.
59. E. H. Lee, A. F. Rowcliffe, and E. A. Kenik, *J. Nucl. Mater.* **83**, 79 (1979).
60. V. Levy, N. Azam, L. Le Naour, G. Didout, and J. Delaplace, in *Proc. Int. Conf. on Radiation Effects in Breeder Reactor Structural Materials*, M. L. Bleiberg and J. W. Bennett (Eds.), Arizona (1977).
61. J. H. Evans, in *Int. Conf. on Irradiation Behaviour of Metallic Materials for Fast Reactor Core Components* (Corsica, 1979).
62. B. A. Loomis, A. Taylor, and S. B. Garber, *J. Nucl. Mater.* **56**, 25 (1975).
63. A. J. E. Foreman, Harwell Report, AERE-R-7135.
64. J. H. Evans, S. Mahajan, and B. L. Eyre, *Phil. Mag.* **26**, 813 (1972).
65. P. B. Johnson and D. J. Mazey, *J. Nucl. Mater.* **91**, 41 (1980); AERE-R-9685.
66. D. Kaletta, *Rad. Effects* **47**, 237 (1980).
67. L. E. Murr, *Science* **183**, 206 (1974).
68. L. E. Murr, *Phys. Stat. Sol. (a)* **22**, 239 (1974).
69. K. Krishan, *Phil. Mag.* **A45**, 401 (1982).
70. A. C. Damask and G. J. Dienes, *Point Defects in Metals*, Ch. 2 (Gordon and Breach, New York, 1963).
71. A. D. Brailsford, R. Bullough, and M. R. Hayns, *J. Nucl. Mater.* **60**, 246 (1976).
72. J. H. Evans, *Scripta Metal.* **10**, 561 (1976).
73. A. D. Brailsford, *J. Nucl. Mater.* **60**, 257 (1976).
74. T. Riste, Noordhoff, *Anharmonic Lattices, Structural Transitions and Melting* (Noordhoff, Leiden, 1974).
75. R. Blinc and B. Zeks, *Soft Modes in Ferroelectrics and Antiferroelectrics* (North-Holland Publishing Co., Oxford, 1974).
76. H. E. Stanley, *Introduction to Phase Transitions and Critical Phenomena* (Clarendon, Oxford, 1971).
77. M. Herschkowitz-Kaufman, *Bull. Math. Biol.* **37**, 585 (1975).
78. A. Goldbeter, *Proc. Nat. Acad. Sci. (USA)* **70**, 3255 (1973).
79. P. Glansdorff and I. Progogine, *Thermodynamic Theory of Structure, Stability and Fluctuations* (John Wiley, New York, 1971).

80. K. Krishan, *Phil. Mag.* **43**, 71 (1981).
81. L. K. Mansur, W. A. Coghlan, and A. D. Brailsford. *J. Nucl. Mater.* **85** and **86**, 591 (1979).
82. J. Keizer, *J. Chem. Phys.* **63**, 398 and 5037 (1975).
83. J. Keizer, *J. Statist. Phys.* **15**, 477 (1976).
84. K. Krishan, *Rad. Effects* **45**, 169 (1980).
85. K. Maleo and R. Bullough, in *Voids Formed by Irradiation of Reactor Materials*, S. F. Pugh, M. H. Loretto and D. I. R. Norris (Eds.), BNES Conf. p. 109 (1971).
86. G. Martin, in *Proc. Int. Conf. on Fundamental Aspects of Radiation Damage in Metals, Vol. 2*, M. T. Robinson and R. W. Young, Jr. (Eds.), CONF-751006, p. 1084 (1975).
87. G. Martin, *Phil. Mag.* **32**, 615 (1975).
88. M. J. Imada, *Phys. Soc. Jap.* **45**, 1443 (1978).
89. J. H. Evans, *J. Nucl. Mater.* **88**, 31 (1980).
90. M. Sachdev and J. Mahanty, *J. Phys.* **C3**, 1225 (1970).
91. D. Sahoo and G. Venkataraman, *Pramana* **5**, 175 and 185 (1975).
92. J. E. Westmorland, J. A. Spragin, F. A. Smidt, and P. R. Malmberg, *Rad. Effects* **26**, 1 (1971).
93. J. Bentley and F. W. Wiffin, in *Proc. 2nd ANS Meeting on Technology of Controlled Nuclear Fusion*, p. 209 (1976).
94. L. D. Hulett, Jr., T. O. Baldwin, J. C. Crump, and F. W. Young, *J. Appl. Phys.* 39, 3945 (1968).
95. J. O. Stiegler and K. Farrell, *Scripta Metal.* **8**, 651 (1974).
96. K. Krishan, in *Proc. Yamada Conference V on Point Defects and Defect Interactions in Metals* (Kyoto, Japan, 1981), in press.
97. K. Krishan and C. Abromeit, to be published.
98. R. Von Jan, *Phys. Stat. Sol.* **8**, 331 (1965).
99. J. Vrijen and S. Radelaar, *Phys. Rev.* **B17**, 409 (1978).
100. W. Wagner, R. Poerschke, A. Axmann, and D. Schwahn, *Phys. Rev.* **B21**, 3087 (1980).
101. H. E. Cook, *Acta Metall.* **18**, 297 (1970).
102. J. W. Cahn, *Acta Metall.* **9**, 795 (1961).
103. J. S. Langer, *Acta Metall.* **22**, 1649 (1973).
104. D. J. Reed, *Rad. Effects* **31**, 129 (1977).
105. E. V. Kornelsen, *Rad. Effects* **13**, 227 (1972).
106. A. Van Veen and L. M. Caspers, Harwell Report, AERE-R 9733, p. 494.
107. B. Viswanathan, private communication.
108. P. Benoist and G. Martin, in *Proc. Int. Conf. on Fundamental Aspects of Radiation Damage in Metals*, Vol. 2, M. T. Robinson and R. W. Young, Jr. (Eds.), CONF-751006, p. 1236 (1975).
109. G. Martin, *Phys. Rev.* **B21**, 2122 (1980).
110. R. Cauvin and G. Martin, in *Proc. Yamada Conference V on Point Defects and Defect Interactions in Metals* (Kyoto, Japan, 1981), in press.
111. R. Cauvin and G. Martin, *Phys. Rev.* **B23**, 3322 and 3333 (1981).
112. C. Abromeit, private communication.
113. J. R. Wills and R. Bullough, *J. Nucl. Mater.* **32**, 76 (1969).
114. A. M. Stoneham, *J. Phys.* **F1**, 778 (1971).
115. V. K. Tewary and R. Bullough, *J. Phys.* **F2**, L69 (1972).
116. V. K. Tewary, *J. Phys.* **F3**, 1275 (1973).
117. L. P. Kubin, A. Rocher, M. O. Ruault, and B. Jouffrey, *Phil. Mag.* **33**, 293 (1976).
118. L. T. Chadderton, E. Johnson, and T. Wohlenberg, in *Proc. of a Conf. on Developments in Electron Microscopy and Analysis* (EMAG 75) (Bristol, 1976).
119. A. I. Rayzanov and L. A. Maksimov, *Rad. Effects* **54**, 195 (1981).
120. W. E. King and R. Benedek, in *Proc. Yamada Conference V on Point Defects and Defect Interactions in Metals* (Kyoto, Japan, 1981), in press.
121. F. V. Nolfi, in *Proc. Int. Conf. on Fundamental Aspects of Radiation Damage in Metals, Vol. 2*, M. T. Robinson and R. W. Young, Jr. (Eds.), CONF-751006, p. 1252 (1975).
122. F. V. Nolfi, *J. Appl. Phys.* **47**, 24 (1976).
123. L. M. Brown, *Scripta Metal* **6**, 387 (1972).
124. D. N. Seidman and R. W. Balluffi, *Scripta Metal* **6**, 789 (1972).
125. D. I. R. Norris and L. M. Brown, *Scripta Metal* **8**, 1045 (1974).
126. A. T. Winter, *Scripta Metal* **7**, 49 (1973).
127. A. A. Lucas, *Phys. Lett.* **41A**, 375 (1972).
128. A. A. Lucas, *Phys. Rev.* **137**, 3527 (1973).
129. A. I. Ryazanov and L. A. Maksimov, *Rad. Effects* **52**, 175 (1980).
130. A. I. Ryazanov and L. A. Maksimov, *Rad. Effects* **55**, 165 (1981).
131. L. A. Maksimov and A. I. Ryazanov, *Rad. Effects* **51**, 197 (1980).

REFERENCES

RADIATION INDUCED ORDERING

BOOKS

1. G. Nicolis and I. Prigogine, *Self-Organization in Non-Equilibrium Systems*, (Wiley-Interscience, 1977).
2. H. Haken, *Synergetics*, (Springer-Verlag, 1978).

REVIEWS & GENERAL READING

1. LIDIARD, A.B
"Statistical Theories of Atomic Transport via Lattice Defects"
Proc. Int. Seminar on "Solute-Defect-Interaction", Kingston
August 1985, to be published by Pergamon Press

2. K. Krishan, *Radiat. Eff.* 66 (1982) 121.
3 K. C. Russell, *Prog. Mater. Sci.* 28 (1984) 229.
4 C. Abromeit, Int. J. Mod. Phys B 2 (1989) 1301-1342
5. H. Wollenberger, in *Physical Metallurgy*, eds. R. W. Cahn and P. Haasen, 3rd edition, 1983, p. 1139.

6 R. E. Howard and A. B. Lidiard, *Rep. Prog. Phys.* 27 (1964) 161.
7. A. R. Allnatt and A. B. Lidiard, *Rep. Prog. Phys.* 50 (1987) 373.

MICROSTRUCTURAL ORDERING

EXPERIMENTAL PAPERS - VOID LATTICE FORMATION

1. J. H. Evans, *Nature* 229, 403 (1971).
2. J. H. Evans, *Rad. Effects* 10, 55 (1971).

3. F. W. Wiffin, in *Radiation Induced Voids in Metals*, J. W. Corbett and L. C. Janniello (Eds.), Albany, USAEC-CONF-71061, p. 386 (1972).

4. J. Moteff, V. K. Sikka, and H. Jang, in *Consultant Symposium, The Physics of Irradiation Produced Voids*,

5. V. K. Sikka and J. Moteff, *J. App. Phys.* 43, 4942 (1972).

6. B. L. Eyre and J. H. Evans, in *Voids Formed by Irradiation of Reactor Materials*, BNES Conf., S. F.

7. J. H. Evans, in *Int. Conf. on Irradiation Behaviour of Metallic Materials for Fast Reactor Core Components* (Corsica, 1979).

8. G. L. Kulcinski and J. L. Brimhall, *Ordered Defect Structures in Irradiated Metals*, ASTM-STP 529, p. 258 (1973).

9. H. Jang and J. Moteff, in *Proc. Int. Conf. on Radiation Effects and Tritium Technology for Fusion Reactors*, J. S. Watson and F. W. Willen (Eds.), CONF-750989, pp. 1–106 (1976).

10. R. S. Nelson (Ed.), AERE-R 7934, p. 181 (1975).
L. J. Chen and A. J. Ardell, *J. Nucl. Mater.* 75, 177 (1978).
B. A. Loomis, S. B. Gerber, and A. Taylor, *J. Nucl. Mater.* 68, 19 (1977).

11 G. L. Kulcinski, J. L. Brimhall, and H. E. Kissinger, *J. Nucl. Mater.* 40, 166 (1971).

12. G. L. Kulcinski, J. L. Brimhall, and H. E. Kissinger, in *Radiation Induced Voids in Metals*, J. W. Corbett and L. C. Ianiello (Eds.), Albany, USAEC-CONF-71061, p. 449 (1972).

13. A. Horsewell & B. N. Singh, Radia. Effects. 102 (1987) 1-5.

EXPERIMENTAL – BUBBLE LATTICE

1. S. L. Sass and B. L. Eyre, *Phil. Mag.* **27**, 1447 (1973).
2. D. J. Mazey, B. L. Eyre, J. H. Evans, S. K. Erents, and G. M. McCraken, *J. Nucl. Mater.* 64, 145 (1977).
3. P. B. Johnson and D. J. Mazey, *J. Nucl. Mater.* 91, 41 (1980); AERE-R-9685.
4. P. B. Johnson and D. J. Mazey, *Nature* 276, 595 (1978).
5. P. B. Johnson and D. J. Mazey, *Rad. Effects* 53, 195 (1980).
6. P. B. Johnson and D. J. Mazey, *J. Nucl. Mater.* 95 and 94, 721 (1980).

EXPERIMENTAL CaF_2 / SrF_2

1. L. T. Chadderton, E. Johnson, and T. Wohlenberg, *Physica Scripta* 13, 127 (1976).
2. L. T. Chadderton, E. Johnson, and T. Wohlenberg, *Rad. Effects* **28**, 111 (1976).
3. L. T. Chadderton, E. Johnson, and T. Wohlenberg, *Comments Sol. State Phys.* **7**, 105 (1976).

EXPERIMENTAL DISLOCATION WALLS

1. W. Jäger, P. Ehrhart and W. Schilling, in *Non-Linear Phenomena in Materials Science*, eds. L. Kubin and G. Martin, *Solid State Phenomena* 3&4 (1988) 279.
2. W. Jäger, P. Ehrhart, W. Schilling, F. Dworschak, A. A. Gadalla, and N. Tsukuda, in *Vacancies and Interstitials in Metals and Alloys*, eds. C. Abromeit and H. Wollenberger, *Mater. Sci. Forum* **15–18** (1987) 881.
3. P. Ehrhart, W. Jager, W. Schilling, F. Dworschak, A. A. Gadalla, and N. Tsukuda in *Mater. Res. Soc. Symp. Proc.* **82** (1987) 265.

MICROSTRUCTURAL ORDERING

Non-Linear Dynamics – Theory

1. K. Krishan, *Nature* **287** (1980) 420.
2. K. Krishan, *Philos. Mag.* **A45** (1982) 401.
3. K. Krishan, in *Non-Linear Phenomena in Materials Science*, eds. L. Kubin *Solid State Phenomena* **3&4** (1988) 267.
4. S. M. Murphy, *Europhys. Lett.* **3** (1987) 1267.
5. S. M. Murphy, in *Materials for Nuclear Reactor Core Applications*, (BNES, 1987), p. 301.
6. S. M. Murphy, in *Non-Linear Phenomena in Materials Science*, eds. L. Kubin and G. Martin, *Solid State Phenomena* **3&4** (1988) 295.
7. E. A. Koptelov and A. A. Semenov, *Phys. Stat. Sol.* **89** (1985) 117.
8. E. A. Koptelova and A. A. Semenov, *Phys. Stat. Sol.* **93** (1986) K33.
9. P. Benoist and G. Martin, in *Proc. Int. Conf. on Fundamental Aspects of Radiation Damage in Metals*, Vol. 2, M. T. Robinson and R. W. Young, Jr. (Eds.), CONF-751006, p. 1236 (1975).
10. A. I. Ryazanov and L. A. Maksimov, *Rad. Effects* 52, 175 (1980).
11. A. I. Ryazanov and L. A. Maksimov, *Rad. Effects* 55, 165 (1981).
12. L. A. Maksimov and A. I. Ryazanov, *Rad. Effects* 51, 197 (1980).
13. J. Keizer, *J. Chem. Phys.* 63, 398 and 5037 (1975).
14. J. Keizer, *J. Statist. Phys.* 15, 477 (1976).
15. K. Krishan, *Rad. Effects* 45, 169 (1980).
16. K. Krishan, *Phil. Mag.* 43, 71 (1981).

MICROSTRUCTURAL ORDERING – OTHER THEORETICAL MODELS

1. J. R. Wills and R. Bullough, *J. Nucl. Mater.* 32, 76 (1969).
2. A. J. E. Foreman, Harwell Report, AERE-R-7135.
3. K. Malen and R. Bullough, in *Voids Formed by Irradiation of Reactor Materials*, S. F. Pugh, M. H. Loretto and D. I. R. Norris (Eds.), BNES Conf. p. 109 (1971).
4. A. M. Stoneham, *J. Phys.* F1, 778 (1971).
5. V. K. Tewary and R. Bullough, *J. Phys.* F2, L69 (1972).
6. V. K. Tewary, *J. Phys.* F3, 1275 (1973).

~~...s of Irradiation Produced Voids, R. S. Nelson~~
~~), AERE-R 7934, p. 319 (1975)~~

~~A. M. Stoneham, in *Proc. Int. Conf. on Fundamental Aspects of Radiation Damage in Metals Vol. 2*, M. T. Robinson and R. W. Young, Jr. (Eds.), CONF-751006, p. 1222 (1975).~~

9 F. V. Nolfi, in *Proc. Int. Conf. on Fundamental Aspects of Radiation Damage in Metals, Vol. 2*, M. T. Robinson and R. W. Young, Jr. (Eds.), CONF-751006, p. 1252 (1975).

10. F. V. Nolfi, *J. Appl. Phys.* 47, 24 (1976).

11 A. J. E. Foreman, Harwell Report, 1972.
12 J. H. Evans, *J. Nucl. Mater.* 119 (1983) 180.
13 J. H. Evans and A. J. E. Foreman, *J. Nucl. Mater.* 137 (1985) 1.
14 J. H. Evans, *J. Nucl. Mater.* 132 (1985) 147.
15 J. H. Evans, in *Vacancies and Interstitials in Metals and Alloys*, eds. C. Abromeit and
16 H. Wollenberger, *Mater. Sci. Forum* 15–18 (1987) 869.

17 J. H. Evans, in *Non-Linear Phenomena in Materials Science*, eds. L. Kubin and G. Martin, *Solid State Phenomena* 3&4 (1988) 303.
18 C. H. Woo and W. Frank, *J. Nucl. Mater.* 137 (1985) 7.
19 C. H. Woo and W. Frank, *J. Nucl Mater.* 140 (1986) 214.
20 C. H. Woo and W. Frank, *J. Nucl Mater.* 148 (1987) 121.
21 C. H. Woo and W. Frank, in *Vacancies and Interstitials in Metals and Alloys*, eds. C. Abromeit and H. Wollenberger, *Mater Sci. Forum* 15–18 (1987) 875.

EXPERIMENTAL – ALLOY ORDERING DURING IRRADIATION

1 Poerschke R, Gölling H W, Wagner W and Wollenberger H 1985 *Mater. Sci. Forum* 3 359
2 Poerschke R, Wagner W and Wollenberger H 1986a *J. Phys. F: Met. Phys.* 16 421
3 Poerschke R, Wagner W, Wollenberger H and Fratzl P 1986b *J. Phys. F: Met. Phys.* 16 1905
4 Poerschke R and Wollenberger H 1976 *J. Phys. F: Met. Phys.* 6 27
5 Wagner W, Ferguson M and Wollenberger H 1987 *Z. Metallk.* to be published
6 Wagner W, Poerschke R and Wollenberger H 1984 *Decomposition in Alloys: The Early Stages (Proc 2nd Acta–Scripta Met. Conf. Sonnenberg)* (New York: Pergamon) p 170
7. Wiedersich H, Okamoto P R and Lam N Q 1979 *J. Nucl. Mater.* 83 98

8. H. R. Brager and F. A. Garner in Effects of Radiation on Materials: Twelfth Conference, ASTM STP 870, F. A. Garner and J. S. Perrin, eds. American Society for Testing and Materials, Philadelphia, PA (1985), pp. 139-150.

1. **GARNER, F.A., BRAGER, H.R., DODD, R.A. and LAURITZEN T.**
Ion-Induced Spinodal-like Decomposition of Fe-Ni-Cr Invar Alloys"
Proc. Int. Seminar on "Solute-Defect-Interaction"
Kingston, August 1985, to be published by Pergamon Press

0. RUSSELL, K.C.
"Phase Stability under Irradiation"
Progress in Material Science, <u>20</u>, 1984, p.229

12 CAUVIN, R. and MARTIN, G.
"Solid Solution under Irradiation :
I.Model for Radiation-Induced Metastability
II.Radiation-Induced Precipitation in AlZn Undersaturated Solid Soluti
III.Further Comments
Phys. Rev., <u>B23</u>, 1981, p.3322 and p.3333 and <u>B25</u>, 1982, p.3385

13 Garner et al. Nucl. Inst. Meth. Phys Res. <u>B16</u> (1986) 244-250
14. T. M. Williams, R. M. Boothby and J. M. Titchmarsh, in *Proc. of Radiation-Induc Sensitisation in Austenitic Steels*, ed. D. I. R. Norris, 1987, p. 116.

ORDERING AND PERIODIC STRUCTURES THEORY

1. G. Martin, *Phys. Rev.* B21 (1980) 2122.
2 G. Martin, *Phys. Rev. Lett.* 50 (1983) 250.

3 R. Sizmann, *J. Nucl. Mater.* 69&70 (1978) 386.

4 C. Abromeit and K. Krishan, *Acta Metall.* 34 (1986) 1515.

5 K. Krishan and C. Abromeit, *J. Phys.* F14 (1984) 1103.

6 E. A. Koptelov, *Phys. Scripta* 35 (1987) 326.
7 C. Abromeit and G. Martin, in *Radiation-Induced Changes in Microstructure*, eds F. A. Garner, N. H. Packan and A. S. Kumar, *ASTM STP* 955 (1987) 822.
8 C. Abromeit and G. Martin, in *Int. Conference on Phase Transformation*, (Ox 1987), p. 350.
9 C. Abromeit and G. Martin, in *Non-Linear Phenomena in Materials Science*, eds
10 L. Kubin and G. Martin, *Solid State Phenomena* 3&4 (1988) 321.
11 S. M. Murphy, *Philos. Mag.* A58 (1988) 417.
12 S. M. Murphy, "Fluctuations in Composition in Dilute Alloys under Irradiation", Harwell Report HL88, 1988.
13 R. Cauvin and G. Martin, in *Solid-Solid Phase Transformations*, eds. H. I. Aaronson,
14 D. E. Laughlin, R. F. Sekera, and C. M. Wayman, (AIME, 1982), p. 281.
15 J. R. Manning, *Diffusion Kinetics for Atoms in Crystals*, (Van Norstrand, 197 p. 95.
16 J. R. Manning, *Phys. Rev.* B4 (1971) 1111.
17 G. Martin and P. Bellon, in *Vacancies and Interstitials in Metals and Alloys*, eds
18 C. Abromeit and H. Wollenberger, *Mater. Sci. Forum* 15–18 (1987) 1337.

19 K. Krishan and C. Abromeit, in *Radiation-Induced Changes in Microstructure* eds. F. A. Garner, N. H. Packan and A. S. Kumar, *ASTM STP* 955 (1987) 809.

20 H. Wiedersich, P. R. Okamoto, and N. Q. Lam, *J. Nucl. Mater.* 83 (1979) 98.

I. W. Chen, *J. Nucl. Mater.* 116 (1983) 249.
W. G. Wolfer, *J. Nucl. Mater.* 114 (1983) 292.
A. Barbu, *Acta Metall.* 28 (1980) 499.
A. R. Allnatt, A. Barbu, A. D. Franklin, and A. B. Lidiard, *Acta Metall.* 31 (1
1307